

## Appendix F

### NONLINEAR ANALYSIS OF ARCH DAMS

#### F-1. Introduction

The example dam is a double-curvature thin arch structure 142.65 m (468 ft) high and 220.68 m (724 ft) long along the crest. The dam is 3.66 m (12 ft) thick at the crest and 15.85 m (52 ft) thick at the base. In this example, the dam is first evaluated using the linear time history analysis for comparison with the damage criteria discussed in Paragraph 6.4d(2). Nonlinear time-history analyses are then performed to obtain quantitative estimates of probable damage in the form of joint opening and lift line cracking for several postulated MCE ground motions.

#### F-2. Purpose and Objectives

The purpose of this example is to illustrate the application of nonlinear time-history method to earthquake response analysis of arch dams. The objectives of this nonlinear time-history analysis are: 1) to model and estimate the amount of contraction joint opening and lift line cracking, 2) to compute displacement and stress response histories of the dam due to six sets of three-component acceleration time histories, and 3) to provide stress contours, stress time histories, and joint displacement time histories for assessing the earthquake performance of the dam.

#### F-3. Scope

The scope of this example includes the following:

- a. Establishment of design earthquake and earthquake ground motions including acceleration time-histories.
- b. Computation of linear earthquake response of the dam-water-foundation system.
- c. Development of nonlinear model with contraction joint opening and lift line cracking.
- d. Computation of earthquake responses of the nonlinear dam model for four sets of acceleration time-histories with various contraction joints and lift lines configurations.
- e. Evaluation of sensitivity of dam response to numbers of contraction joints and lift line joints.
- f. Evaluation of sensitivity of dam response to characteristics of acceleration time histories.

#### F-4. Earthquake Ground Motions

For evaluation of the earthquake damage using linear and nonlinear time-history analyses, the example arch dam was assumed to be located in the near field of a maximum earthquake event having a moment magnitude  $M_w$  of about 6-1/2. A total of six sets of records were selected for the analysis, five of which included natural acceleration time-histories from four recent earthquakes, and the sixth consisted of a spectrum-matched time-history derived using the 1971 Pacoima Dam record. The smooth response spectra for the horizontal and vertical components of ground motion were constructed to be representative of median ground motions for an  $M_w$  6-1/2 earthquake occurring at a distance of  $R \approx 5$  km (3.1 miles). The records

considered are listed in Table F-1 and the smooth response spectra are shown in Figure F-1. The ground motions were scaled such that the sum of ordinates for the response spectra of each natural record would match the sum for the smooth response spectra in the period range of 0.1 to 0.5 sec. This period range was selected to contain the most significant modes of vibration for the example dam (i.e., all periods longer than 0.1 sec). The resulting scale factor for each record is listed in Table F-1, and the response spectra for all records in the period range of 0.1 to 0.5 sec are compared in Figure F-2. Time-histories of the larger horizontal component of the records are plotted in Figure F-4. This figure clearly demonstrates the pulsive (“fling”) type motions contained in the Pacoima Dam and Morgan Hill records.

<b>Table F-1. Near-Source Earthquake Records</b>		
<b>Earthquake Record</b>	<b>Designated Name</b>	<b>Scale</b>
Coyote Lake Dam 1984 Morgan Hill earthquake, $M_w$ 6.2, R = 0.1 km	CLD	0.64
Gilroy Array No. 1 1989 Loma Prieta earthquake, $M_w$ 6.9, R = 11 km	GLY	0.81
Spectrum-matched 1971 Pacoima Dam record	PACB	1.00
Pacoima Dam, downstream record 1994 Northridge earthquake, $M_w$ 6.7, R = 8 km	PACN	1.13
Pacoima Dam, downstream record 1971 San Fernando earthquake, $M_w$ 6.6, R = 2.8 km	PACX	0.52
Newhall, West Pico Canyon Boulevard 1994 Northridge earthquake, $M_w$ 6.7, R = 7.1 km	U56	1.80

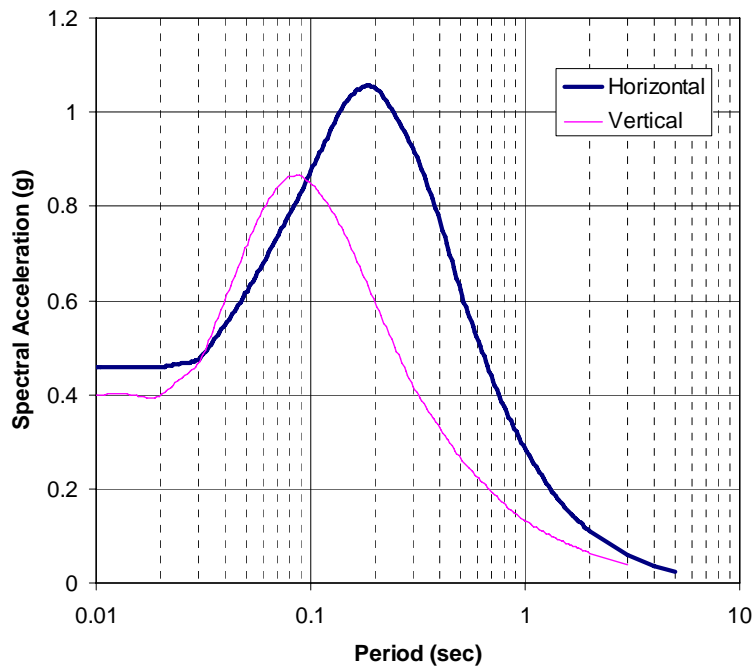


Figure F-1. Horizontal and vertical smooth response spectra

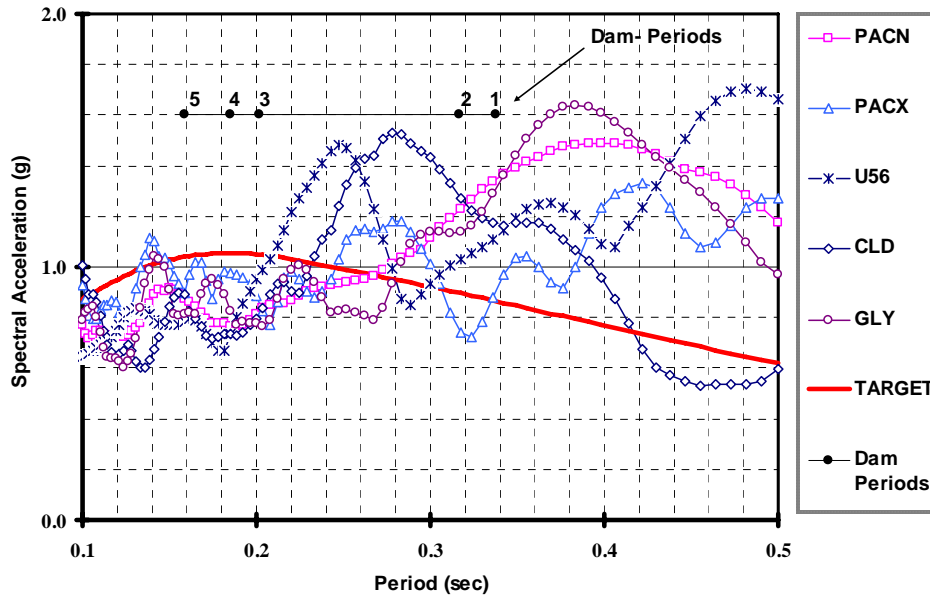


Figure F-2. Response spectra of scaled records

### F-5. Computation of Linear-elastic Response

The linear-elastic time-history analysis of the example dam is based on the 3-D finite-element procedures discussed in Chapter 2 of EM 1110-2-6051. Finite-element models for the concrete arch, foundation rock, and the impounded water were developed using the GDAP program and loading combinations were established in accordance with EM 1110-2-2201. Material properties were selected from the available data. The ground motion acceleration time history inputs for the dynamic analysis were selected based on the procedures discussed in Chapter 5 of EC 1110-2-6051. Interaction effects of the impounded water and foundation rock with the dam were included in the finite-element stress analyses by modeling a sufficiently large portion of the foundation rock and the impounded water. A 5% structural damping ratio was assumed in the analyses.

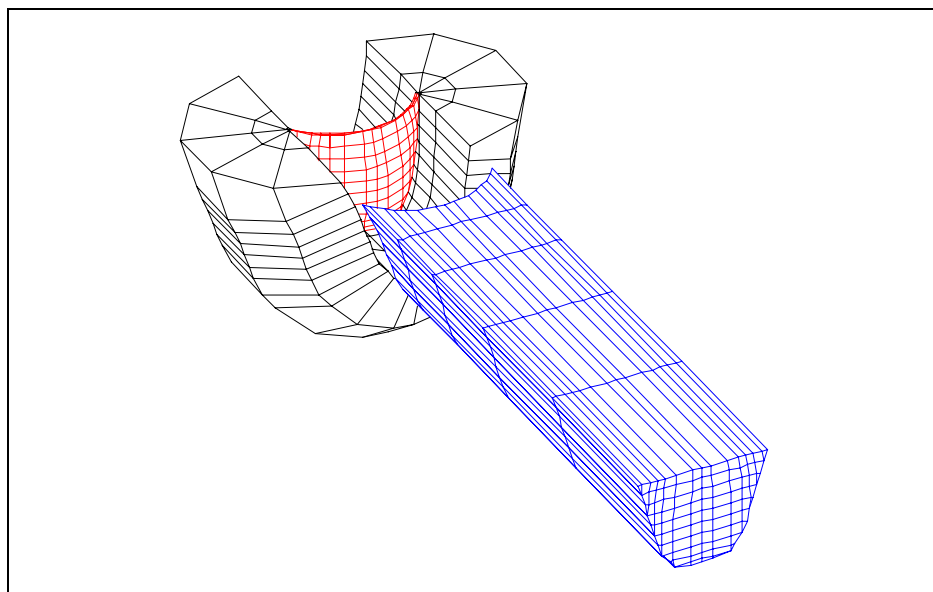


Figure F-3. Three-dimensional view of dam-rock-reservoir system

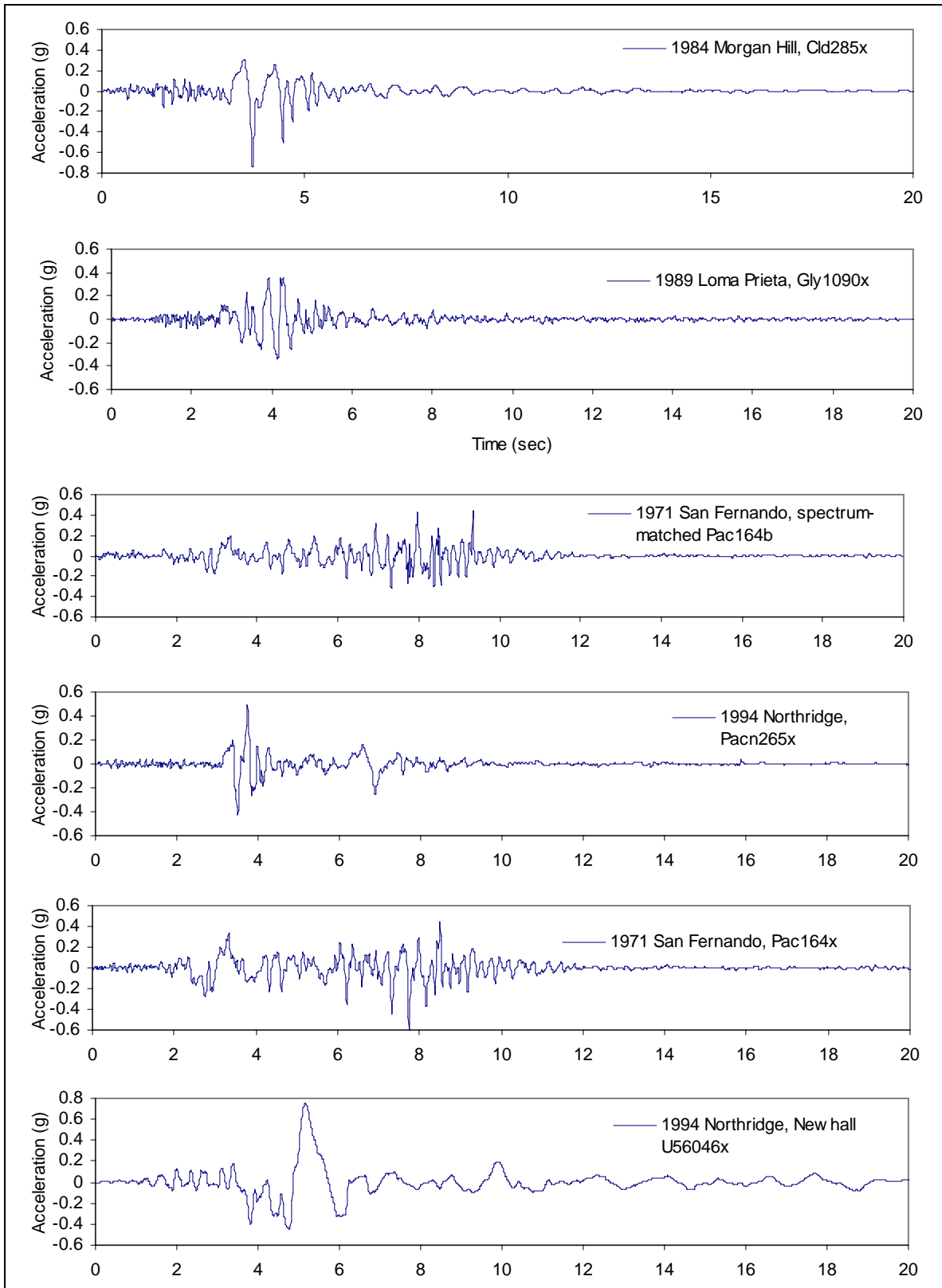


Figure F-4. Scaled acceleration time-histories for near-source,  $M_w \sim 6\text{-}1/2$  earthquake

### F-6. Evaluation of Linear-elastic Analyses Results

The dam-water-foundation model in Figure F-3 was analyzed for six sets of three-component acceleration time histories discussed above in Section F-4. The Web-based GDAP program (Quest Structures 2001), a three-dimensional finite-element program for linear-elastic analysis of concrete dams was used. The results are presented and evaluated with the damage criteria in Paragraph 6.4d(2). Figure F-5 compares the magnitude and extent of high arch and high cantilever tensile stresses with the performance curves established for arch dams (see Chapter 4 of EM 1110-2-6051). The upper graphs show that the surface areas and cumulative inelastic duration of arch tensile stresses exceed the permissible values set for the linear-elastic analysis. The lower graphs show that the surface areas of cantilever tensile stresses are below the permissible values but their cumulative inelastic duration exceeds the permissible values. The results suggest that the nonlinear response of the dam in the form of contraction joint opening and lift line cracking is significant and well above the established threshold. Therefore, the evaluation of dam safety should proceed with nonlinear analysis including contraction joint opening and lift line cracking.

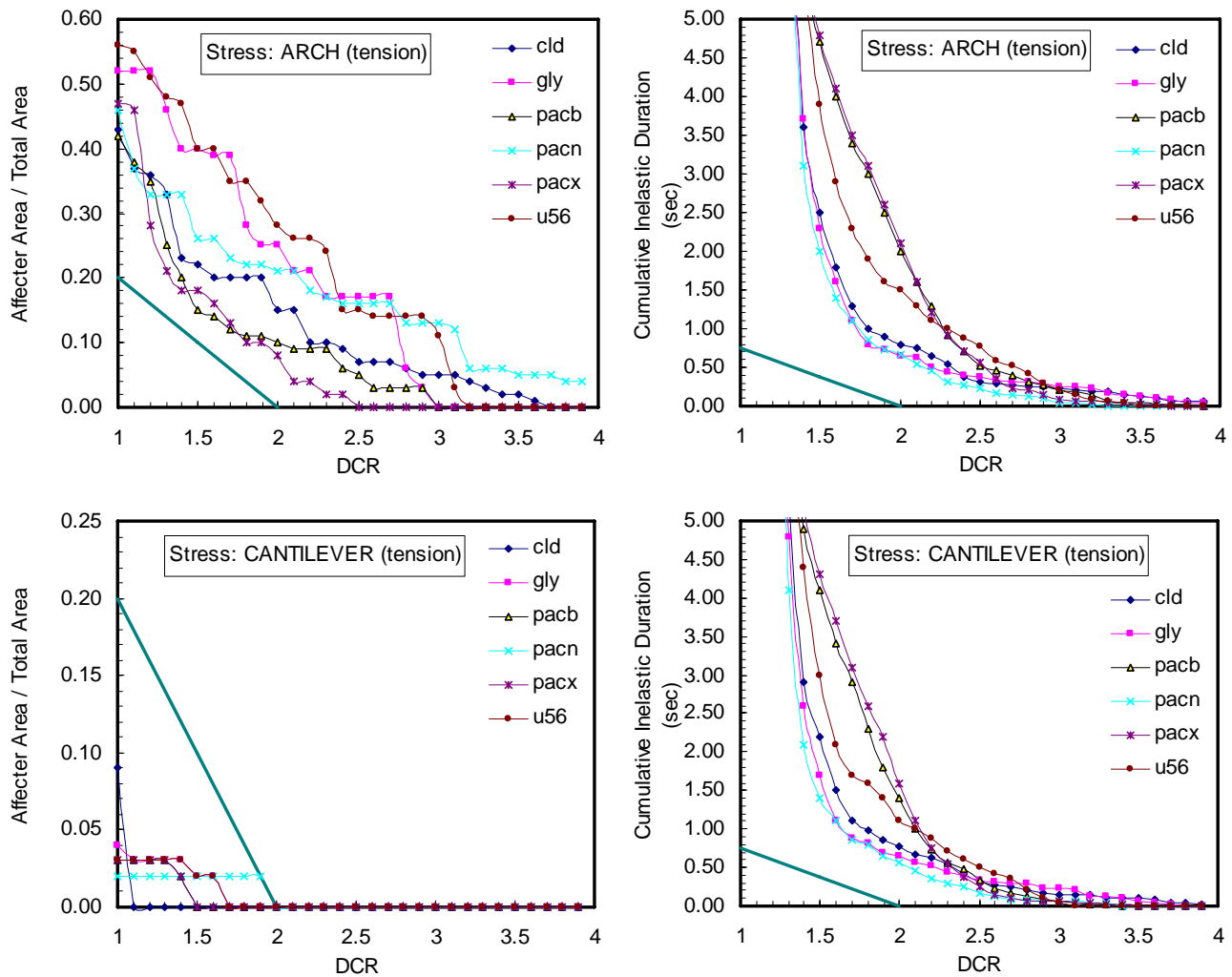


Figure F-5. Performance evaluation curves for Morrow Point Dam

## F-7. Selection of Nonlinear Analysis Procedures

The results of linear analyses indicated that the high tensile arch stresses are well above the tensile strength of contraction joints and would lead to significant joint opening requiring nonlinear analysis. The Web-based dam analysis program QDAP was used to perform earthquake nonlinear analyses for the example arch dam ([www.WebDams.com](http://www.WebDams.com)). QDAP is a 3D finite-element nonlinear analysis program with capabilities to account for nonlinear effects due to opening and closing of contraction joints and cracking/opening of lift lines during the earthquake ground shaking. The program uses a substructure technique to reduce the amount of computational effort. In substructure technique nonlinear equations of motion are formed only for the degrees of freedom at the contraction joints, or at the dam-foundation interface. Each cantilever bounded by the contraction joints and dam-rock abutment is considered as a substructure behaving in a linear manner under static and dynamic loads. The foundation rock is also a linear substructure in the entire system. The hydrodynamic loads are represented by the added mass terms. Any opening of the joints under hydrostatic and temperature loads are also considered in the analysis. QDAP is an enhanced version of the ADAP-88 program developed at UC Berkeley (Fenves et. al, 1989).

## F-8. Nonlinear Finite-element Model

a. Nonlinear earthquake response of an arch dam is sensitive to the modeling assumptions and characteristics of the earthquake ground motion. In this example several analyses are conducted to examine the effects that numbers and configuration of joints and characteristics of earthquake acceleration time histories might have on response of the dam. The finite-element model of the dam system will include the body of the dam, several contraction joints and lift lines represented by nonlinear joint elements, a portion of the foundation rock, and inertia effects of the impounded water represented by added mass terms. The analysis will start with three vertical contraction joints and proceed with more contraction joints and lift lines, as appropriate.

b. *Dam Model.* The dam model is developed using mesh generation capability of the GDAP program. The body of the dam is modeled similar to that used in the linear-elastic analysis. It includes three layers of 8-node solid elements through the dam thickness. The 8-node solid elements are three-dimensional isoparametric elements with linear geometry and displacement interpolation in three directions. The finite-element mesh of the dam is arranged along horizontal and vertical planes to facilitate modeling of the joints. The vertical planes are oriented in the radial direction same as the contraction joints. This way, when needed, nonlinear joint elements can easily be inserted along the horizontal lift lines and the vertical contraction joints. A total of 270 8-node solid elements, 90 elements in each of the three layers were used to model the body of the dam, as shown in Figure F-6.

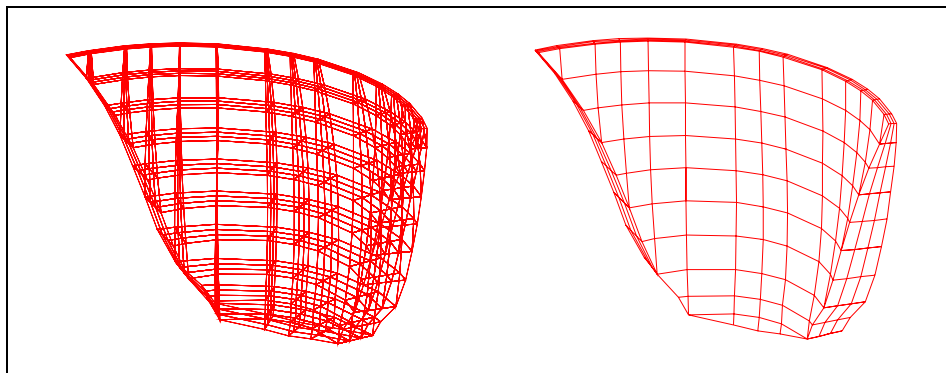


Figure F-6. Finite-element mesh of dam body

c. *Nonlinear Joint Model.* Concrete arch dams are constructed as individual cantilever blocks separated by vertical contraction joints. The contraction joints usually are grouted at the completion of the dam or in stages and may also include shear keys for additional resistance. However, contraction joints have limited tensile resistance and can open and close repeatedly during the earthquake ground shaking that produces net tensile forces across the joints. Such opening and closing of the joints is transient in nature, but if severe, can lead to unstable cantilever blocks and concrete crushing due to impact. The joint opening relieves tensile stresses across the joint but compressive stresses are increased due to the impact and reduced contact surfaces. This nonlinear behavior therefore needs to be investigated to ensure that the amount of joint opening and compressive stresses are not excessive. The contraction joint opening is modeled using a nonlinear joint element shown in Figure F-7 (Fenves et al., 1989). The nonlinear joint element consists of two coincident surfaces, each defined by four nodes that may lie on a plane (Figure F-7a). The element stiffness properties, displacements, and stresses are computed at four Gauss integration points shown in Figure F-7b. The relative displacements between the two element surfaces,  $v$ , produce stresses,  $q$ , according to the nonlinear relationship described in Figure F-7c. As shown in this figure, the element is characterized by the tensile strength,  $q_0$ , and the stiffness,  $k$ . The tensile strength  $q_0$  can be selected to represent different joint types. For example,  $q_0 = 0$  represents an ungrouted joint or a grouted joint with zero tensile strength. Whereas a nonzero  $q_0$  represents a grouted joint for which some tensile strength can be assumed. Finally, a large value of  $q_0$  may be used to simulate a linear analysis for which the joints are not permitted to open. The nonlinear joint elements are placed between cantilever blocks to model opening and closing of contraction joints, between lift lines to model cracking and opening and closing of the lift lines, and at the dam-foundation contact to model cracking and separation of the dam from the foundation.

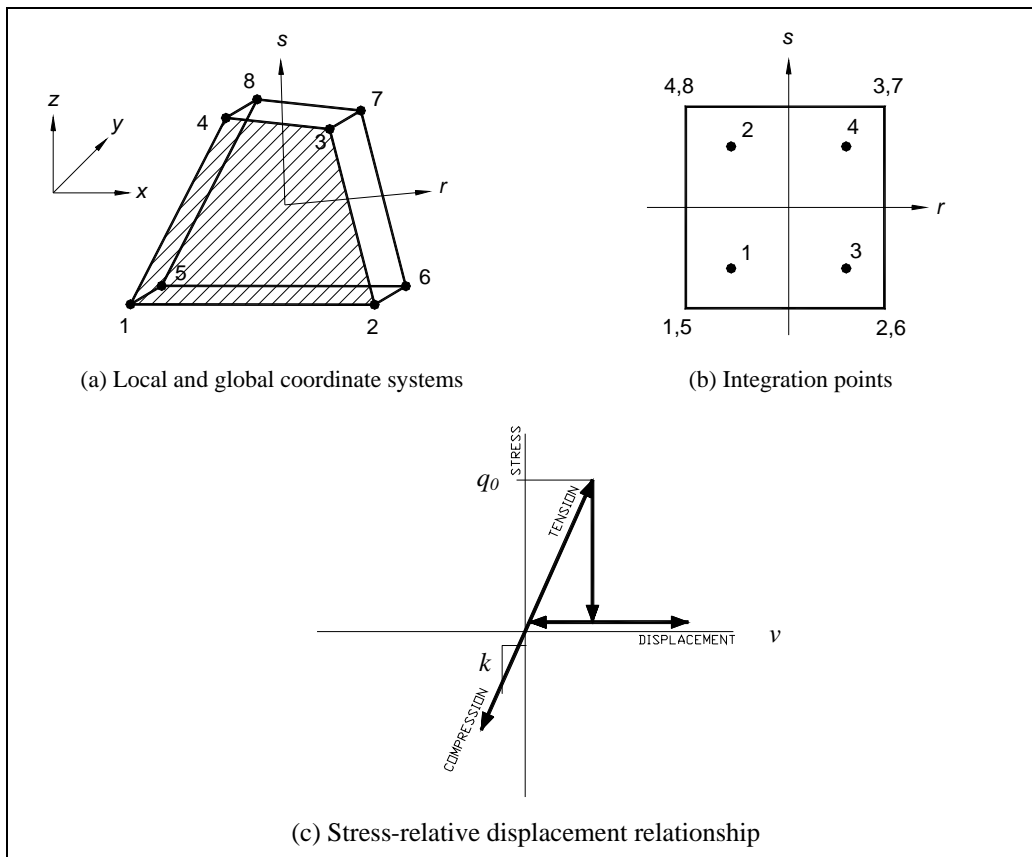


Figure F-7. Nonlinear Joint Element

d. *Foundation Model.* The finite-element model of the foundation rock is similar to that used in the linear analysis and shown in Figure F-3. The finite-element mesh for the foundation was constructed on the semi circular planes cut into the canyon wall perpendicular to the dam-foundation interface. The radius of the semi-circle was selected twice the dam height. A total of 396 8-node solid elements were used. The foundation model was assumed to be massless, an assumption that is commonly used in practice to eliminate reflection of seismic waves at the fixed boundaries of the foundation model and to apply the earthquake records measured at the ground surface directly at the base of the foundation model.

e. *Incompressible Water Model.* The inertia forces of the impounded water due to earthquake shaking were represented by the equivalent added mass terms applied to the upstream nodes of the dam. The added-mass of water was computed using a finite-element mesh of incompressible water, as shown in Figure F-3. The fluid mesh, which was developed in the linear analysis, included five element layers and was constructed by projecting the upstream nodes of the dam about five times the water depth in the upstream direction. This prismatic fluid mesh included a total of 450 3D fluid elements to represent the body of the water and 90 2D fluid elements to establish the dam-water interface. The water level was assumed at the crest elevation. The computer program QRES ([www.WebDams.com](http://www.WebDams.com)) was used for solution of the incompressible added mass. The resulting added-mass is a full matrix that couples all degrees-of-freedom at the upstream face of the dam. If left this way, this matrix couples all substructures together, thus negating the major advantage of the substructure solution for the joint opening mechanism. For this reason, the added-mass matrix is diagonalized in the nonlinear analysis using QDAP.

## F-9. Selection of Nonlinear Analysis Parameters

a. As mentioned earlier, the nonlinear earthquake response of arch dams is sensitive to the numbers and configuration of the joints as well as on characteristics of the earthquake ground motion. In this example both of these issues are examined. With respect to joint opening three models are considered: 1) a model with three vertical contraction joints, 2) a model with five vertical contraction joints, and 3) a model with five vertical contraction joints, two lift-line joints, and a peripheral joint at the dam-foundation contact. The sensitivity to ground motion is addressed by using six sets of three-component acceleration time histories with a wide range of ground motion characteristics including the near field effects. Other analysis parameters such as the concrete and foundation rock material properties, joint properties, and damping are kept the same for all eighteen analyses.

b. *Material Properties.* Material properties for the concrete and foundation rock are listed in Table F-2 below. Whenever applicable they are given for both the static and dynamic loading to account for the effects of rate of loading on modulus values and material strengths. A nominal compressive strength of 3,000 psi was assumed for the concrete. Note that the foundation rock is assumed not to be affected by thermal loading; thus a coefficient of thermal expansion of zero is assigned to the rock. Furthermore, the unit weight of the rock is set to zero to satisfy the assumption of massless foundation discussed earlier.

**Table F-2. Assumed material properties**

<b>Concrete Material Properties</b>				
Static Compressive Strength	$(f_c')_{st}$	4,000.00	psi	27.50 MPa
Dynamic Compressive Strength	$(f_c')_d$	5,000.00	psi	34.50 MPa
Static Tensile Strength	$(f_t)_{st}$	450.00	psi	3.10 MPa
Apparent Dynamic Tensile Strength	$(f_t)_{ad}$	900.00	psi	6.2 MPa
Modulus of Elasticity (static)	$E_{st}$	454,700.00	ksf	21,771.00 MPa
Modulus of Elasticity (Dynamic)	$E_d$	604,800.00	ksf	28,958.00 MPa
Coefficient of Thermal Expansion	$\alpha$	5.00E-06		5.00E-06
Unit Weight	$\gamma$	0.15	kcf	2402.77 Kg/m <sup>3</sup>
Poisson's Ratio	$\nu$	0.20		0.20
<b>Rock Material Properties</b>				
Modulus of Elasticity	$E$	460,800.00	ksf	22,063.00 MPa
Coefficient of Thermal Expansion	$\alpha$	0.00		0.00
Unit Weight	$\gamma$	0.00	kcf	0.00 kcf
Poisson's Ratio	$\nu$	0.20		0.20

*c. Joint Properties.* The joint properties needed for the analysis are the normal stiffness and tangential stiffness with the corresponding joint strengths. The normal and tangential stiffness for the joint element are assigned large values to enforce displacement continuity at the contraction joints. However, these values should not be too large to cause numerical problems. Appropriate stiffness values for the joint may be selected equal to  $(n.E/L)$  where  $E$  is the modulus of elasticity of the concrete and  $L$  is the length of the adjacent 3D solid element in the direction normal to the joint. Depending on the floating point precision,  $n$  may range from 10 to 100 with larger values for higher precision floating point representation. In this example a stiffness value of  $157 \times 10^9$  N/m<sup>3</sup> ( $1 \times 10^9$  lb/ft<sup>3</sup>) was assumed in the normal and tangential directions. The joint strength ( $q_0$ ) was set to zero assuming that the joint cannot resist any tension.

*d. Damping.* QDAP requires that proportional Rayleigh damping be used. Ten modes of vibration were used to approximate 5% critical damping for the concrete dam. The periods of vibration needed for this purpose were computed using the GDAP program.

*e. Number and Configuration of Joints.* Three joint configurations were analyzed. Initially three vertical contraction joints were modeled at the location of maximum tensile arch stresses from the linear analysis. These locations were at the quarter span points and at the crown section of the dam. Each of these contraction joints was modeled by many nonlinear joint elements that covered the entire length of the joint from the top to bottom and through the thickness of the dam. Based on the results of this initial model, a second configuration with five contraction joints was analyzed. The locations of these joints were also selected on the basis of tensile arch stresses. A third and final configuration included three types of joints: five vertical, two horizontal, and one peripheral joint at the dam-foundation interface. The purpose of the vertical joints was to relieve high tensile arch stresses. The horizontal joints were to permit cracking and opening of the lift lines experiencing excessive tensile cantilever stresses; while the peripheral joint was intended to relieve tensile stresses at the dam-foundation contact caused by the assumption of linear-elastic behavior. Additional joints may be used to redistribute the joint openings. However, too many joints can significantly affect the computation time.

## F-10. Computation of Nonlinear Earthquake Response

### a. Analysis with Three Contraction Joints (Model 1)

(1) *Description of Model.* The nonlinear analysis for joint opening should start with a minimum number of contraction joints at the locations of maximum tensile arch stresses. The stress results from the linear-elastic analysis show that high tensile arch stresses develop on the upstream face at the crown section and on the downstream face near the quarter span points (see Figure 4-18 in EM 1110-2-6051). Thus the obvious choice is to start with three vertical contraction joints, one at the crown section and one each at the ¼ span points, as shown in the upstream view of the dam in Figure F-8 below. In this figure the thick lines indicate the locations where the nonlinear joint elements will be inserted. The addition of contraction joints increases number of nodal points, but the number of three-dimensional solid elements remains the same. A total of 72 contraction joint elements were used in this model.

(2) *Results.* The analysis began with the application of gravity, hydrostatic, and temperature loads as the initial conditions, followed by the step-by-step nonlinear time-history dynamic analysis for the seismic loads. Results are summarized in Table F-3 and in Figures F-9 to F-14 for the six input acceleration time history records. The table shows the maximum amount of joint opening with the peak tensile and peak compressive stresses. The figures display deflected shapes at the time of maximum joint opening, time-history of the maximum joint opening, envelopes of maximum arch and cantilever stresses, and vector plots of maximum principal stresses for the upstream and downstream faces of the dam. As expected, the maximum joint opening occurs at the crown section. Table F-3 indicates that the maximum joint opening varies from 1.2 inches for the spectrum-matched 1971 Pacoima Dam record (PACB) to 3.36 inches for the Gilroy record of 1989 Loma Prieta earthquake (GLY). The contraction joint at the crown-section opens 8 to 20 times during the ground shaking provided by six different acceleration time-history records. The 20 openings occur during the application of the spectrum-matched 1971 Pacoima Dam record (PACB). This confirms that the spectrum-matched records tend to increase the number of strong motion cycles. Each joint opening cycle lasts between 0.1 to 0.2 seconds, except for the Newhall record of 1994 Northridge earthquake (U56) during which the joint stays open about 0.5 second (Figure F-14). The reason for this long-duration opening is the presence of the long-period acceleration pulse in the Newhall record (Figure F-4). The results also show that tensile arch stresses have significantly reduced but not vanished. Therefore, it appears more contraction joints could be beneficial. In the next analysis, the number of contraction joints were increased to five, as discussed in Paragraph F-10b.

**Table F-3. Summary of maximum joint opening and stresses for case with three contraction joints**  
(1 MPa = 145 psi)

Ground Motion Record	Max. Displ (in)	Max. Joint Opening (in)	Peak Tensile stresses (psi)			Peak Compressive Stresses (psi)		
			Arch	Cantilever	Principal	Arch	Cantilever	Principal
CLD	5.31	1.56	910	976	1,752	-3,451	-3,359	-3,932
GLY	9.67	3.36	1,193	1,008	1,679	-3,394	-2,395	-3,574
PACB	4.62	1.20	799	792	1,265	-2,509	-2,139	-3,349
PACN	5.83	1.38	907	881	1,537	-3,119	-2,290	-3,703
PACX	8.07	2.40	1,204	899	1,743	-3,490	-2,584	-4,014
U56	8.95	2.88	680	979	1,169	-2,648	-3,294	-3,404

**Table F-4. Summary of maximum joint opening and stresses for case with five contraction joints**  
(1 MPa = 145 psi)

Ground Motion Record	Max. Displ (in)	Joint Opening (in.)	Peak Tensile stresses (psi)			Peak Compressive Stresses (psi)		
			Arch	Cantilever	Principal	Arch	Cantilever	Stress
CLD	5.63	1.56	1,028	1,315	1,441	-2,536.	-1,964	-3,478
GLY	10.02	2.58	897	1,193	1,852	-3,526	-2,439	-3,584
PACB	4.60	1.08	1,331	756	1,338	-2,715	-2,027	-3,311
PACN	5.80	1.44	1,017	1,046	1,430	-3,225	-2,510	-3,754
PACX	8.23	2.16	1,162	936	1,641	-3,385	-2,667	-4,051
U56	8.61	2.15	869	990	1,140	-2,711	-3,295	-3,598

**Table F-5. Summary of maximum joint opening and stresses for case with vertical, horizontal, and peripheral joints** (1 MPa = 145 psi)

Ground Motion Record	Max. Displ. (in)	Joint Opening (in.)	Peak Tensile stresses (psi)			Peak Compressive Stresses (psi)		
			Arch	Cantilever	Principal	Arch	Cantilever	Principal
CLD	5.99	1.80	846	994	1,208	-2,576	-1,890	-2,638
GLY	10.59	4.32	1,308	1,365	2,113	-3,094	-2,089	-3,355
PACB	5.43	1.98	823	786	1,355	-2,038	-1,719	-2,202
PACN	6.26	2.40	1,223	1,186	1,822	-3,352	-1,944	-3,629
PACX	9.75	3.72	1,187	1,408	2,023	-3,198	-1,922	-3,256
U56	15.35	9.50	1,117	1,438	2,300	-3,758	-1,994	-3,759

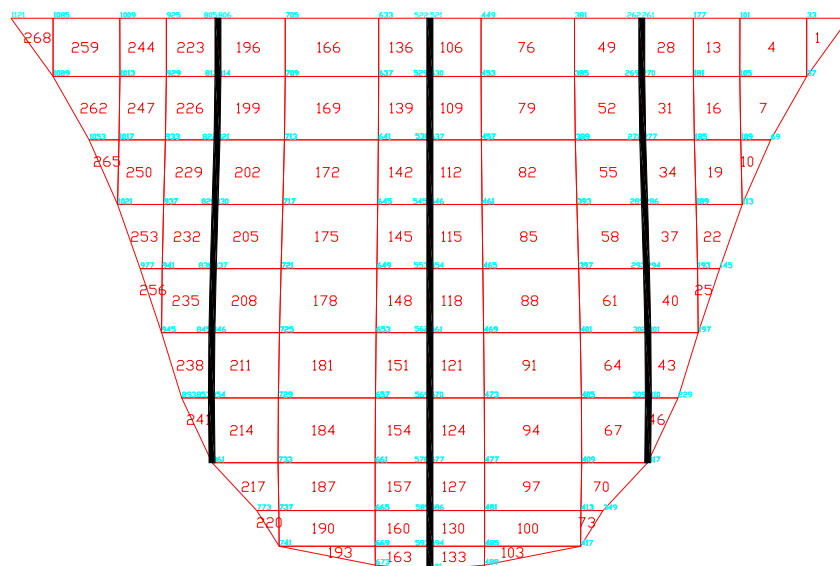


**Figure F-8. Finite-element mesh with three contraction joints (Model 1)**

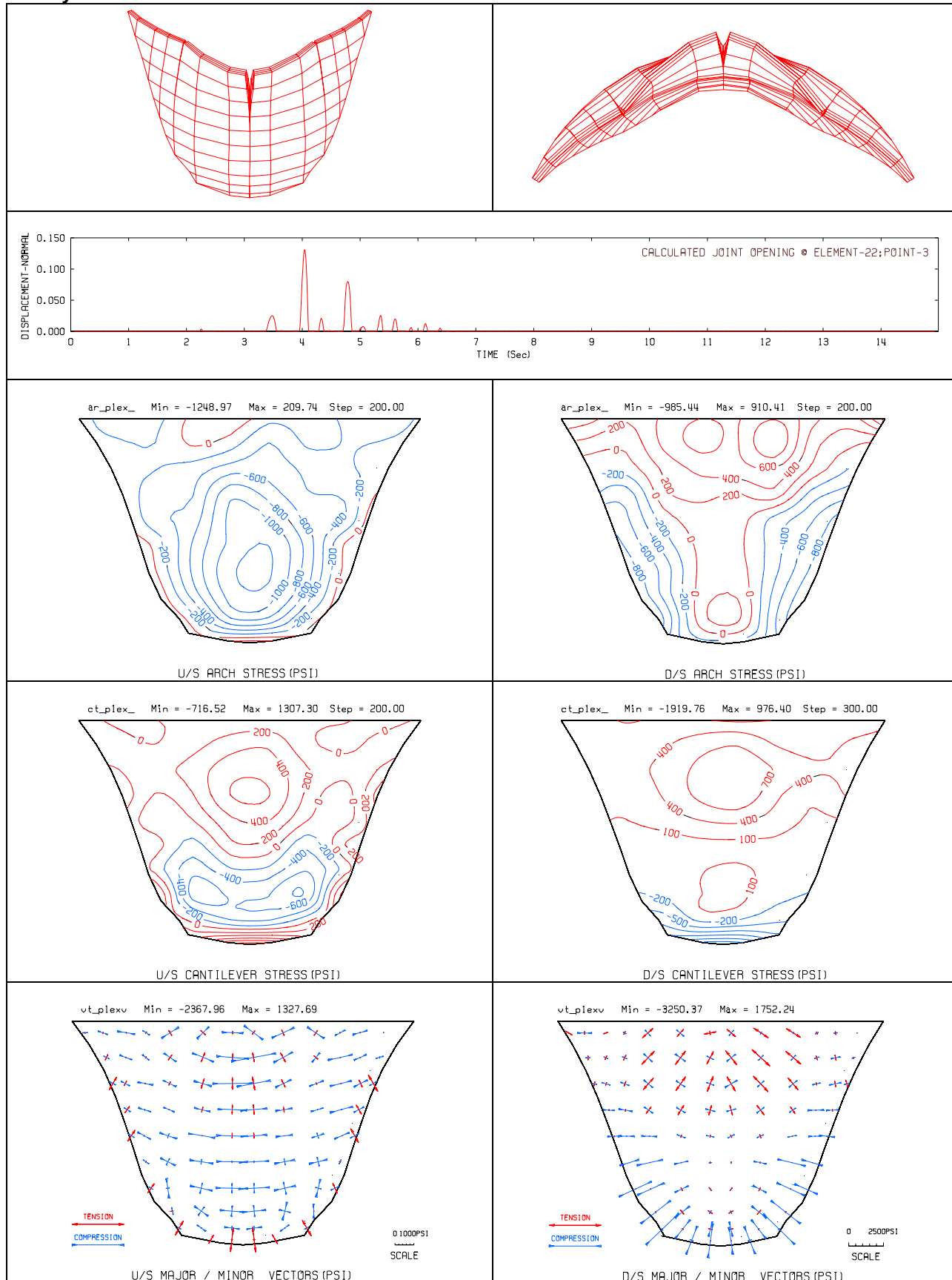


Figure F-9. Deflected shapes, maximum joint opening time history (in units of ft), envelopes of maximum arch and cantilever stresses, & envelopes of principal stress vectors due to CLD record

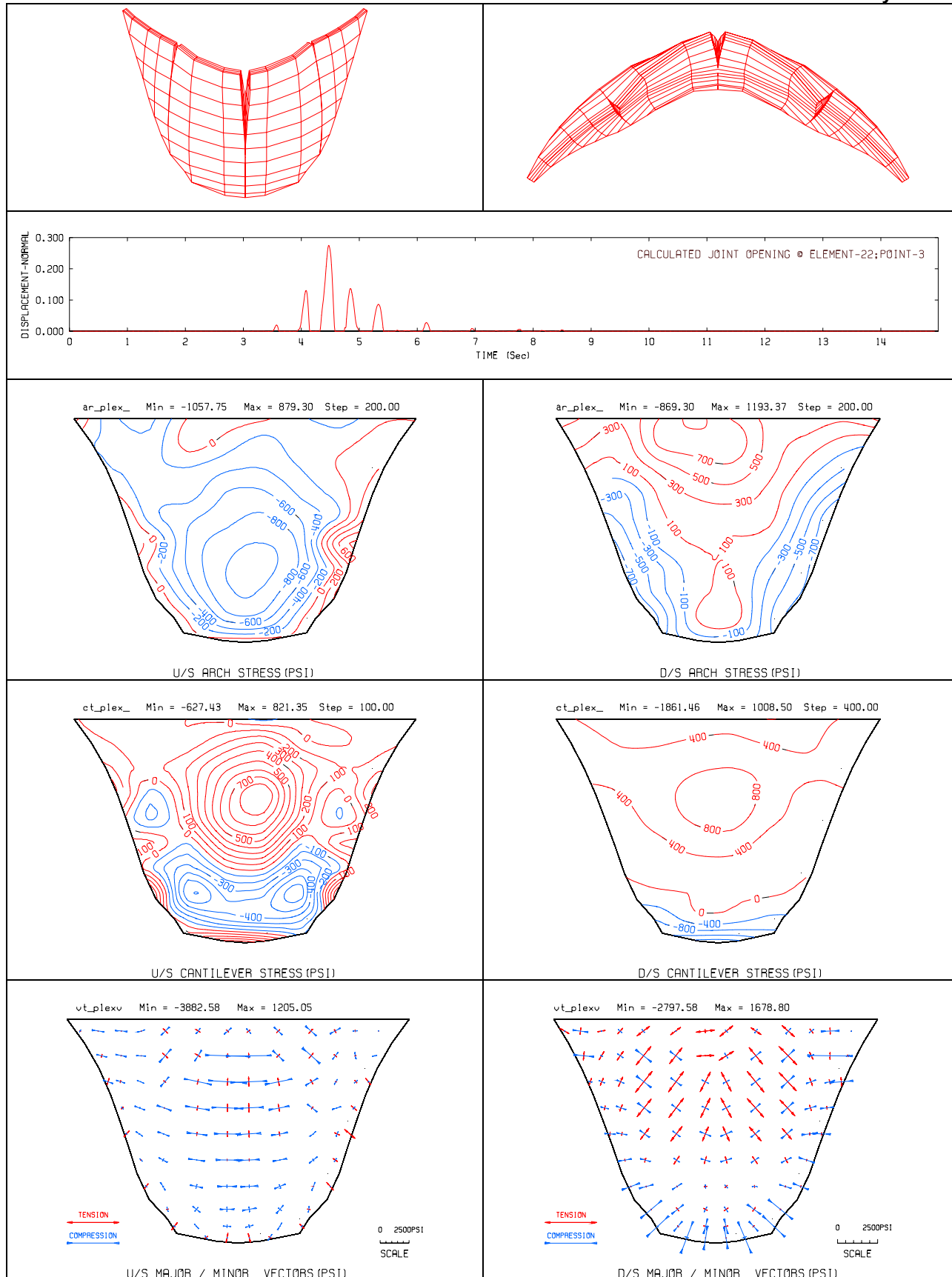


Figure F-10. Deflected shapes, maximum joint opening time history (in units of ft), envelopes of maximum arch and cantilever stresses, & envelopes of principal stress vectors due to GLY record

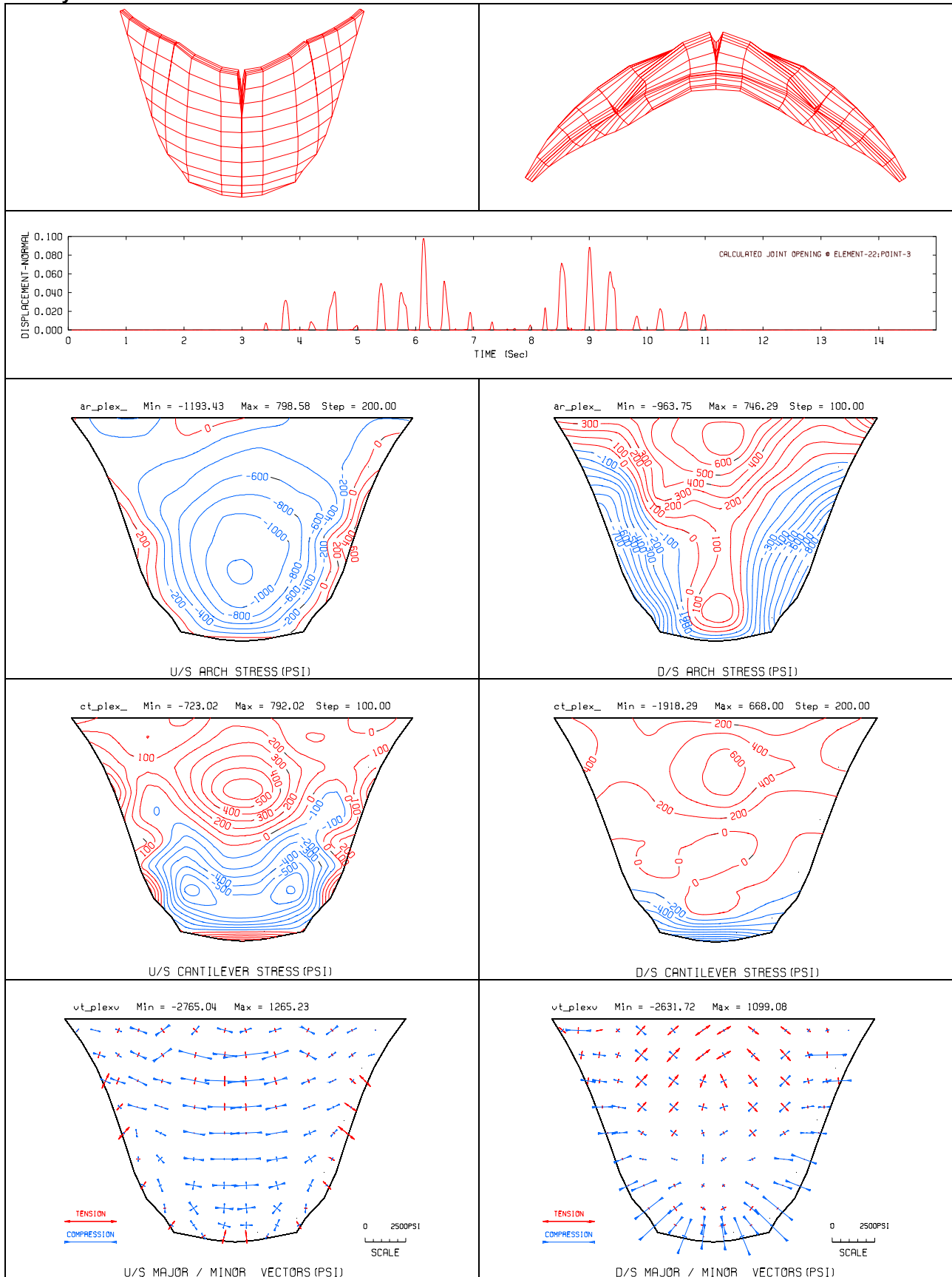


Figure F-11. Deflected shapes, maximum joint opening time history (in units of ft), envelopes of maximum arch & cantilever stresses, & envelopes of principal stress vectors due to PACB record

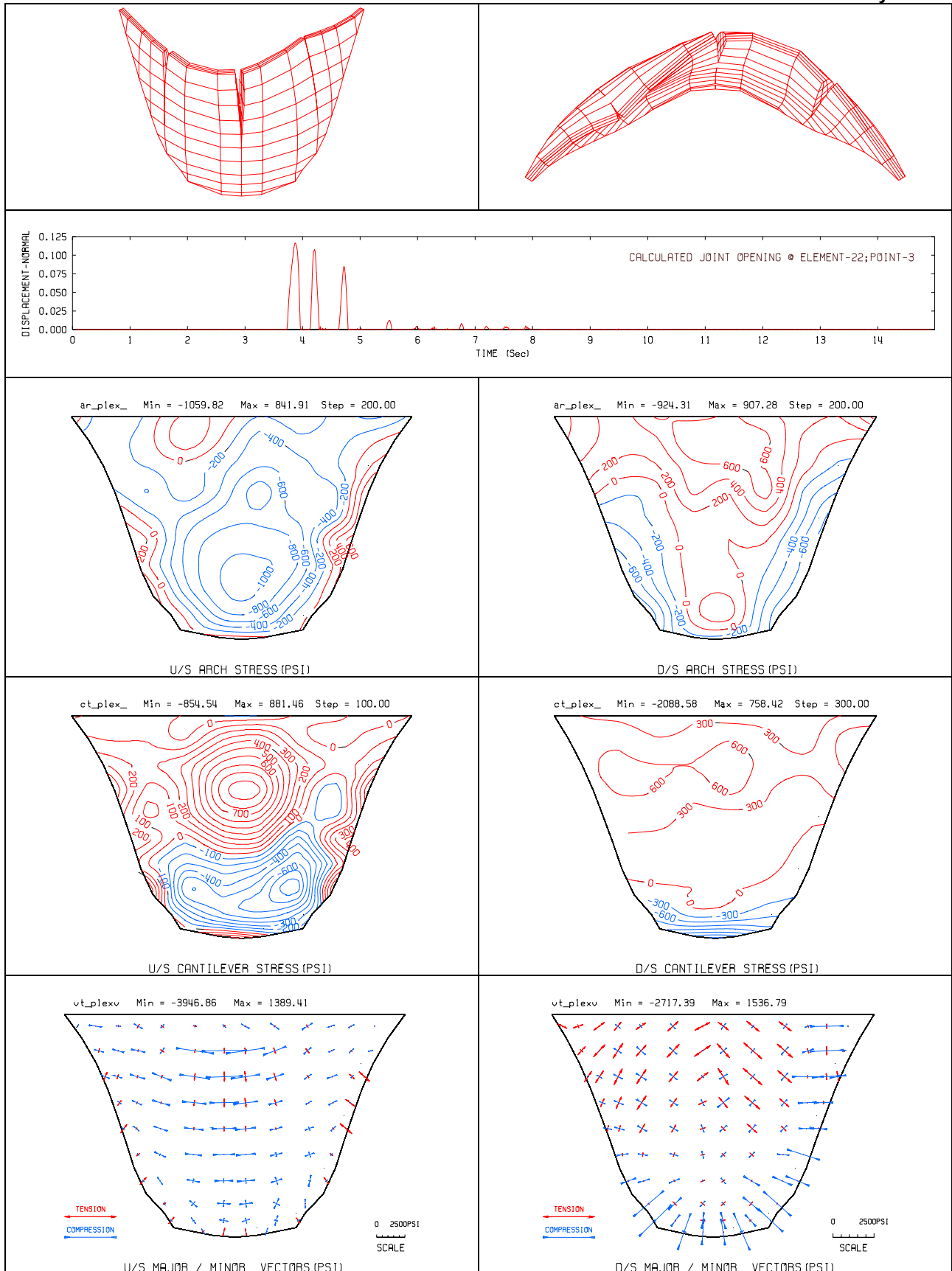


Figure F-12. Deflected shapes, maximum joint opening time history (in units of ft), envelopes of maximum arch & cantilever stresses, & envelopes of principal stress vectors due to PACN record

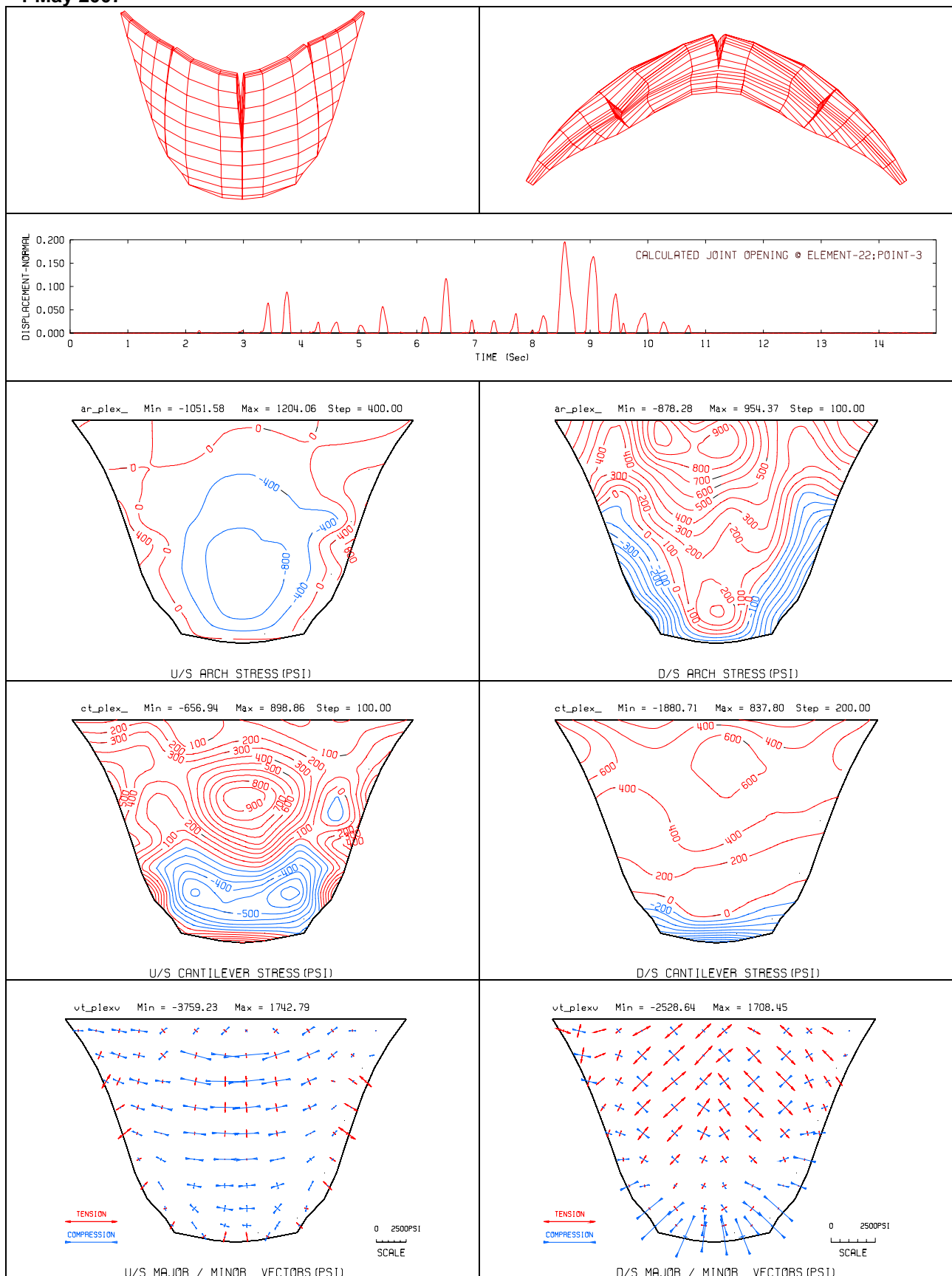


Figure F-13. Deflected shapes, maximum joint opening time history (in units of ft), envelopes of maximum arch & cantilever stresses, & envelopes of principal stress vectors due to PACX record

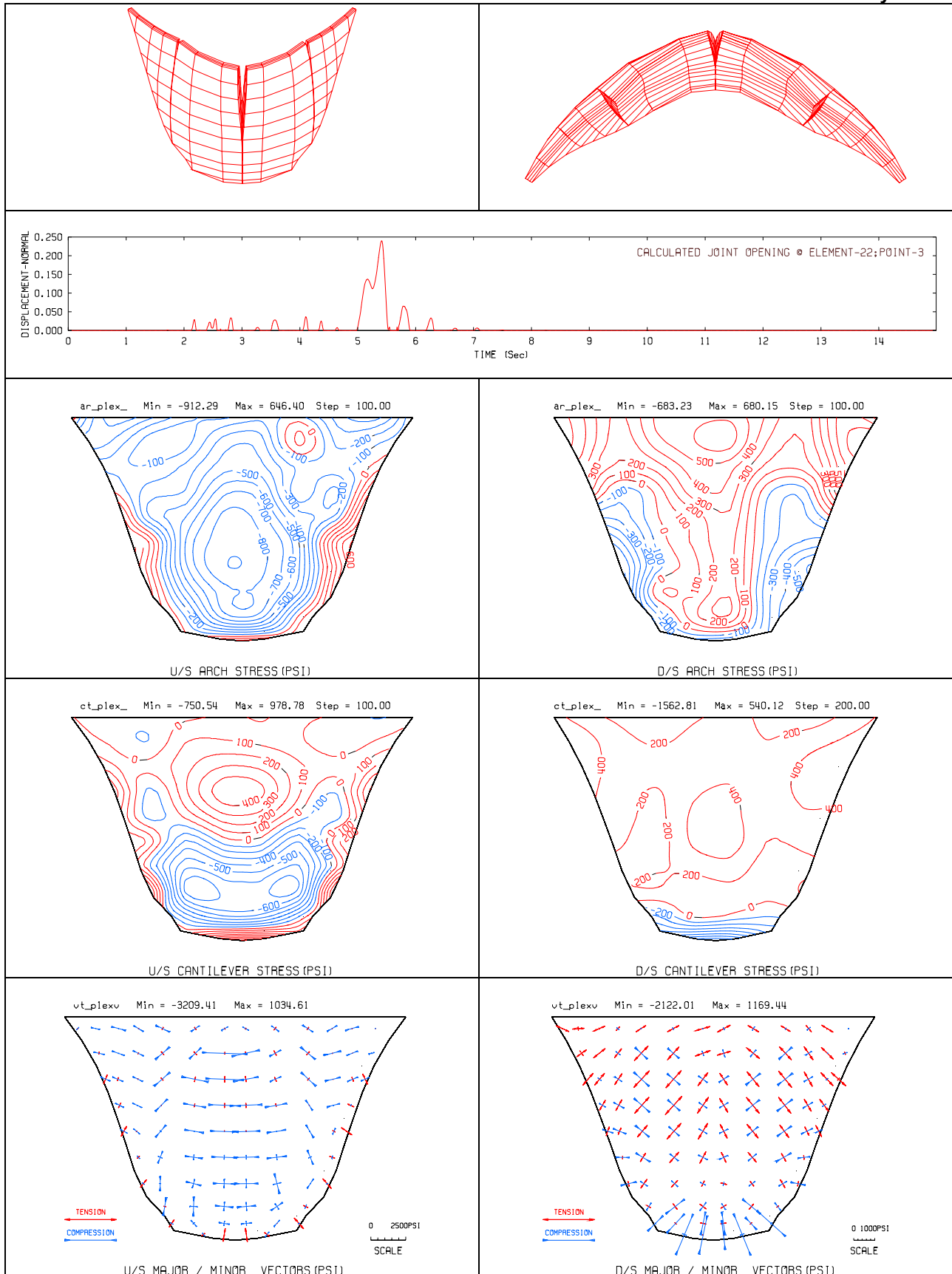


Figure F-14. Deflected shapes, maximum joint opening time history (in units of ft), envelopes of maximum arch and cantilever stresses, & envelopes of principal stress vectors due to U56 record

b. Analysis with Five Contraction Joints (Model 2)

(1) *Description of Model.* The finite-element model with five contraction joints is shown in Figure F-15. The contraction joints were distributed uniformly along the length of the dam. A total of 114 contraction joint elements were employed.

(2) *Results.* Again the analysis began with the application of static loads as the initial conditions, followed by the step-by-step nonlinear time-history dynamic analysis for the selected six earthquake records. The results are summarized in Table F-4 and in Figures F-16 to F-21. Overall, the results for the five-contraction-joint model (Model-2) are similar to those for the three-contraction-joint model (Model-1), except that the amounts of maximum joint openings are 4 to 25 percent smaller. The largest joint opening still occurs for the Gilroy record (GLY), except that at 2.58 inches the Model-2 joint opening is 23% smaller than the 3.36 inches computed for Model-1 (Tables F-3 and F-4). The joint opening reduction for Newhall record (U56) is about 25 percent. The stress magnitudes have increased for some input records and decreased for others showing no obvious tendencies. The changes in stress magnitudes are mostly limited to 0.7 to 1.4 MPa (100 to 200 psi), which are not large. In summary there are no significant differences between the responses of Model-1 and Model-2. However, Model-2 which distributes joint openings to more contraction joints is preferable and will be used in conjunction with the lift joints and peripheral joints in the next section.

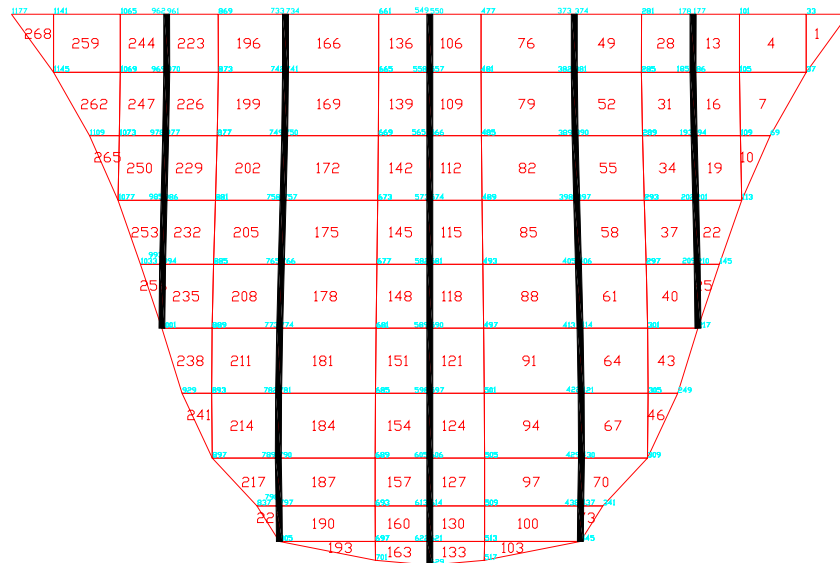


Figure F-15. Finite-element mesh with five contraction joints (Model 2)

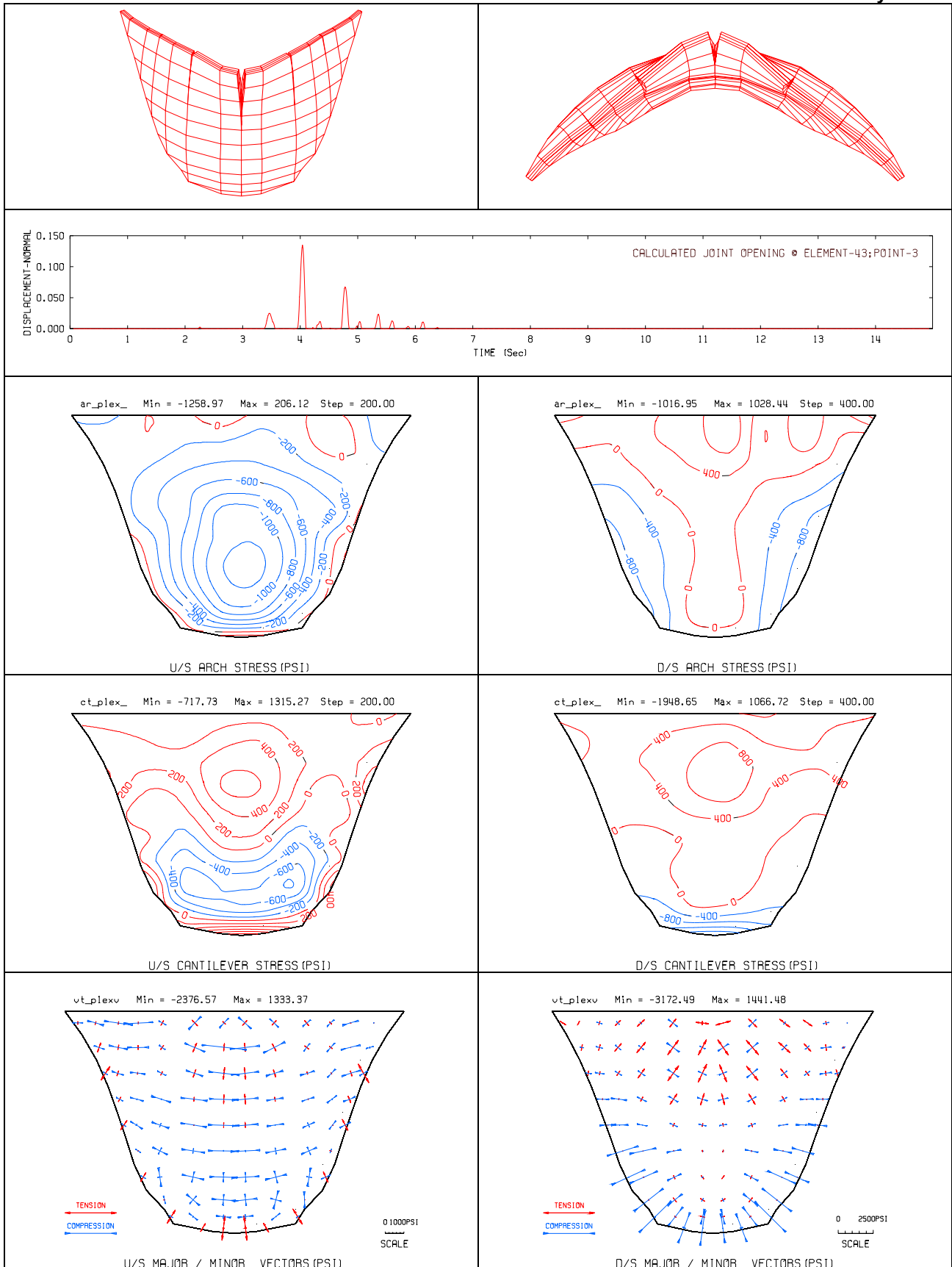


Figure F-16. Deflected shapes, maximum joint opening time history, envelopes of maximum arch and cantilever stresses, and envelopes of principal stress vectors due to CLD record

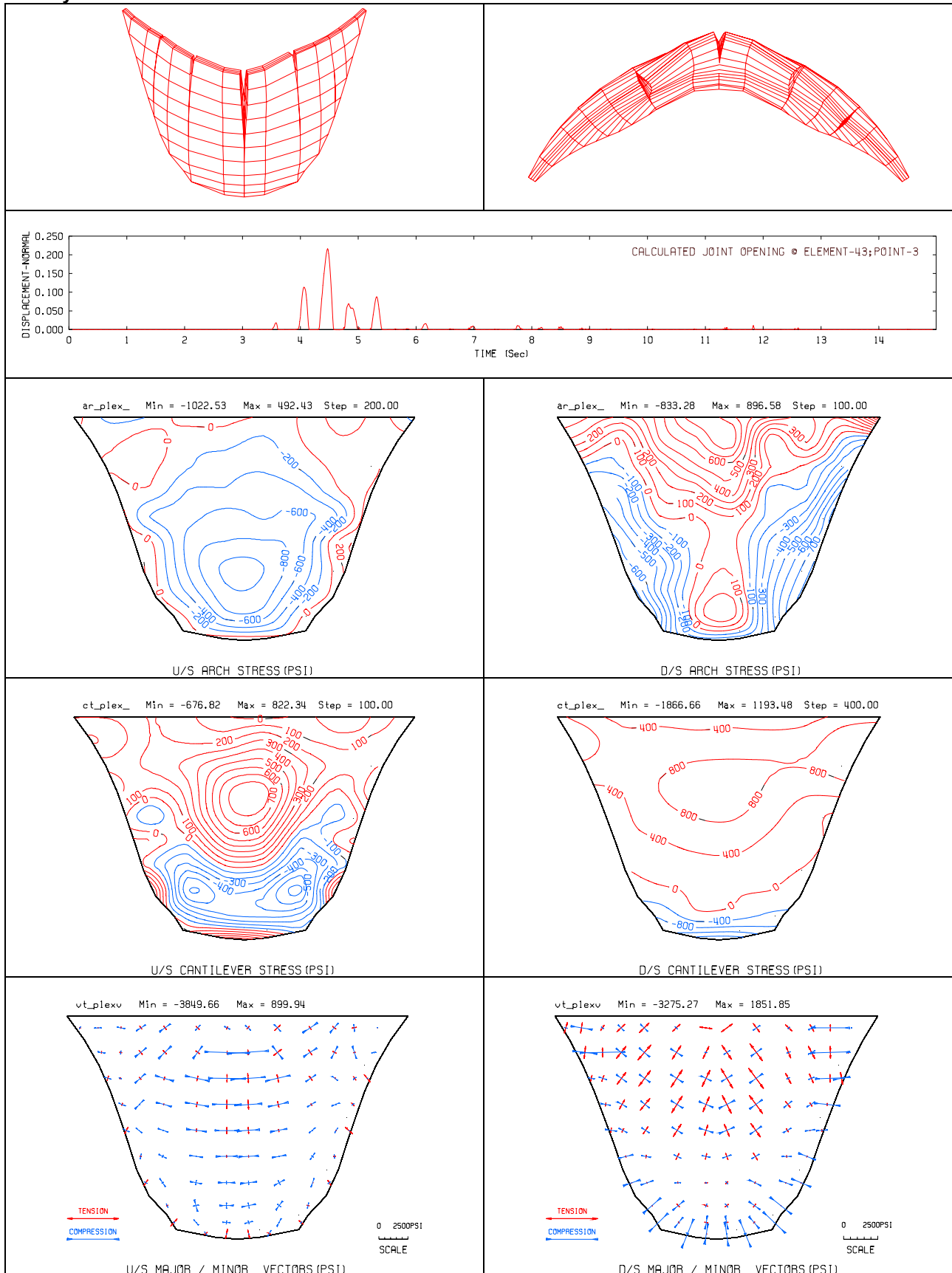


Figure F-17. Deflected shapes, maximum joint opening time history, envelopes of maximum arch and cantilever stresses, and envelopes of principal stress vectors due to GLY record

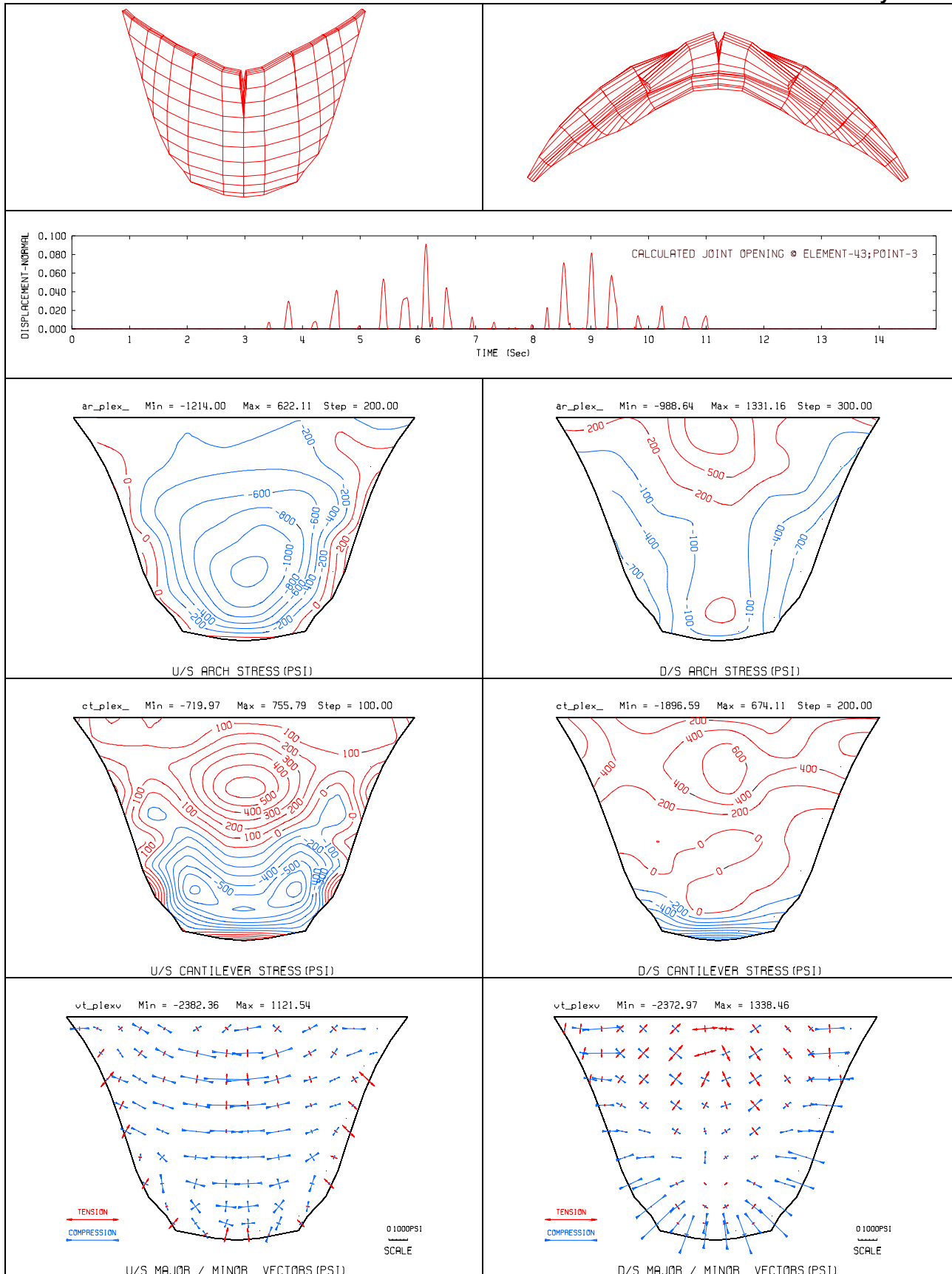


Figure F-18. Deflected shapes, maximum joint opening time history, envelopes of maximum arch and cantilever stresses, and envelopes of principal stress vectors due to PACB record

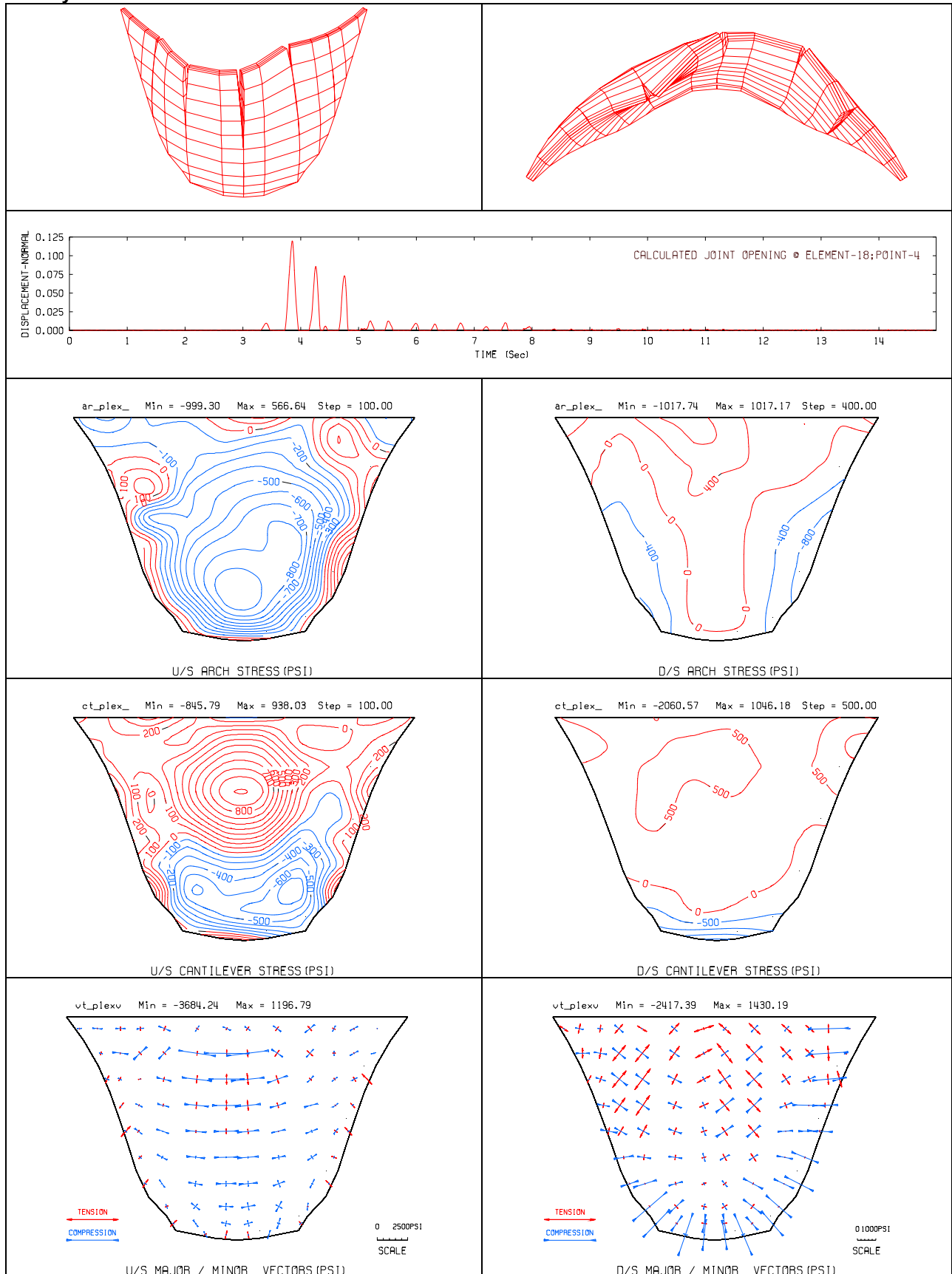


Figure F-19. Deflected shapes, maximum joint opening time history, envelopes of maximum arch and cantilever stresses, and envelopes of principal stress vectors due to PACN record

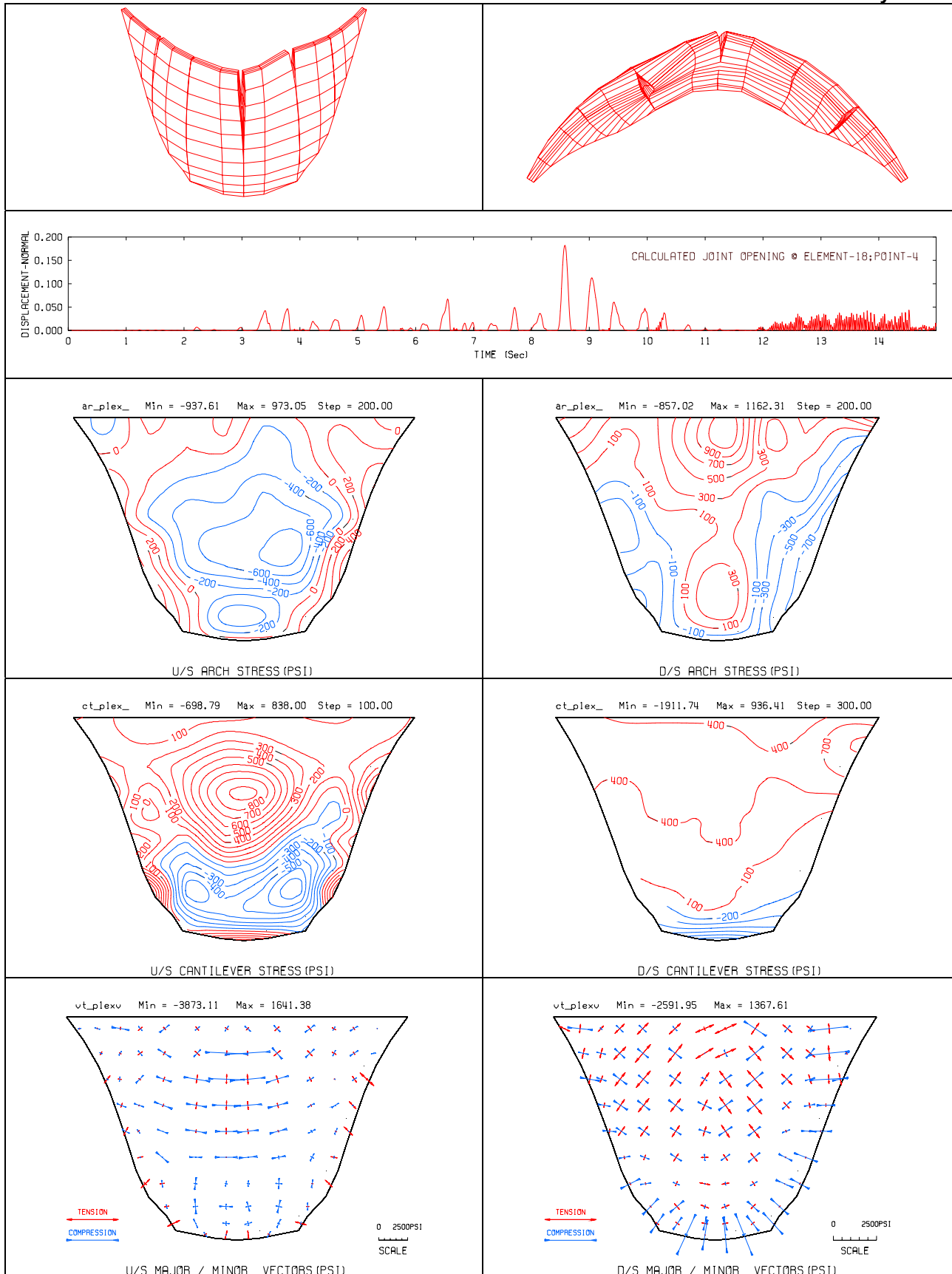


Figure F-20. Deflected shapes, maximum joint opening time history, envelopes of maximum arch and cantilever stresses, and envelopes of principal stress vectors due to PACX record

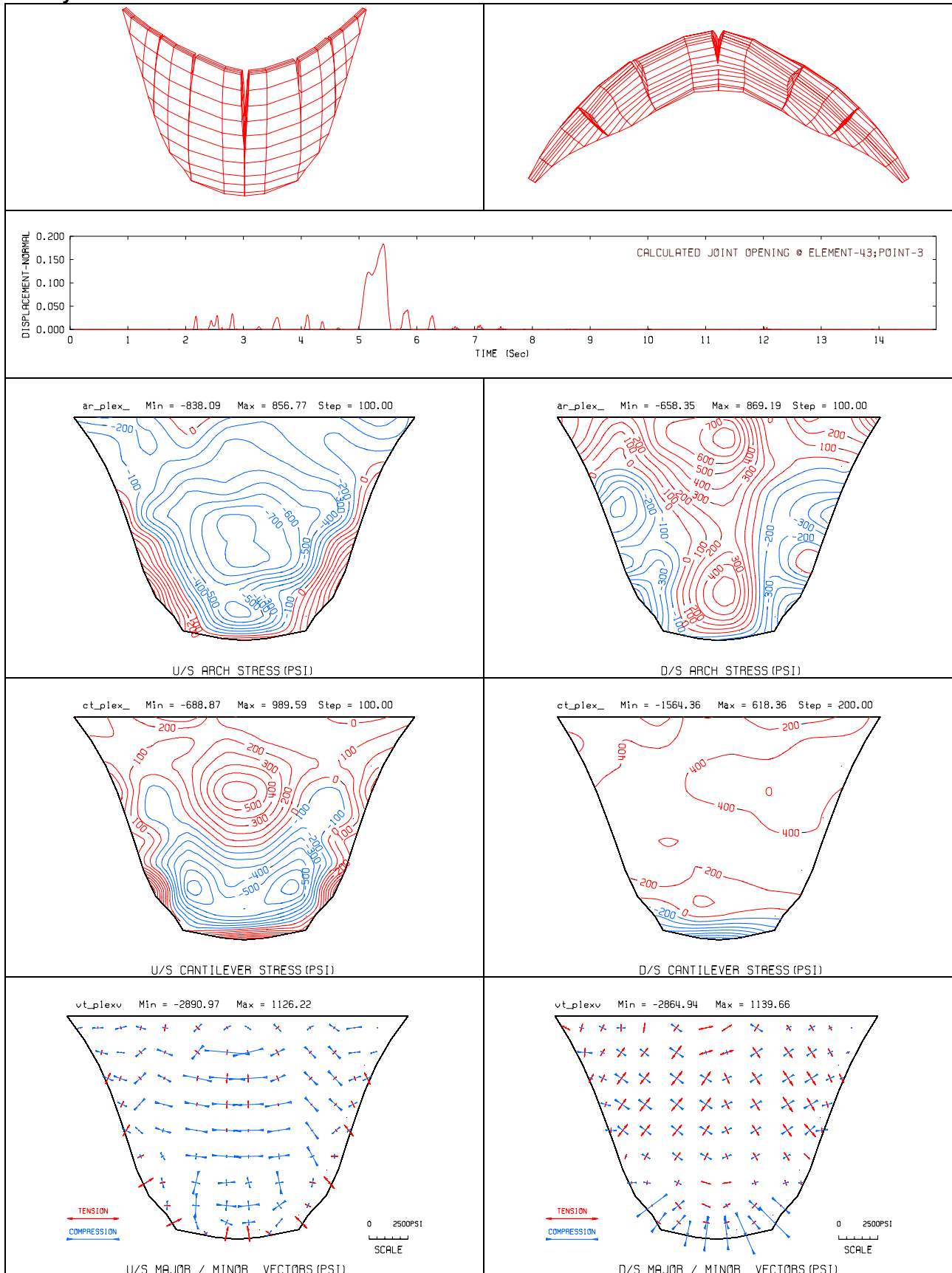


Figure F-21. Deflected shapes, maximum joint opening time history, envelopes of maximum arch and cantilever stresses, and envelopes of principal stress vectors due to U56 record

*c. Analysis with Vertical, Horizontal, and Peripheral Joints (Model 3)*

(1) *Description of Model.* The results of Model 2 with five contraction joints showed that high tensile stresses still persist within the cantilever blocks isolated by the opened contraction joints and along the dam-foundation contact. Model 3 with five vertical, two horizontal, and the peripheral joints was constructed to study the effects of tensile cracking that may occur at the lift joints and at the dam-foundation contact. As shown in Figure F-22, Model 3 employs the same vertical joints used in Model 2 with two additional horizontal joints at the location of high cantilever stresses and one peripheral joint at the dam-foundation contact. Each of these joints includes three nonlinear elements through the dam thickness and matches the number of solid elements on the faces of the dam. A total of 240 nonlinear joint elements were used.

(2) *Results.* The results for the static plus seismic loads are summarized in Table F-5 and in Figures F-23 to F-28 for the six selected input acceleration time-histories. The maximum dam radial displacements and joint openings listed in Columns 2 and 3 of Table F-5 indicate significant increase in the amount of joint opening, especially for the Newhall record (U56). In addition, Figures F-23 to F-28 show that the joint openings not only are larger for Model 3 but the joints stay open for a longer period. This is because Model 3 is more flexible and vibrates at a longer period than the other two models. Consequently, opening and closing of the joints occur at a slower rate. Another observation is that modeling of the lift lines has also changed mechanism of the nonlinear joint opening. For example, the deflected shape in Figure F-25 exhibits two dislocated blocks at the top of the dam that are isolated by the contraction joint openings on both sides and the bottom lift line. Furthermore, Figure F-26 demonstrates a mechanism where the top and bottom part of the dam are separated through an opened lift line, while the contraction joints apparently remain closed. The largest joint opening reaches 9.5 inches for the Newhall record (U56). Such a large joint opening could affect stability of the dam and will be investigated in the next section. Although stress results indicate that tensile stresses at the contraction joints and lift lines have vanished, they are still persistent within the blocks and have somewhat increased compared to the results for Model 1 and Model 2. The reason for this is the tangential constrain enforced by the joint elements that precludes any joint slippage and thus induces tensile stresses within the blocks. Such constraint is a shortcoming of QDAP program that need to be removed. The results also show the magnitudes of compressive stresses that are usually higher than those computed in the linear analysis. The maximum compressive stresses are approaching the static compressive strength of 27.5 MPa (4,000 psi) but are less than the dynamic compressive strength of 34.5 MPa (5,000 psi) . Nevertheless some minor concrete crushing can be expected to occur as a result of impact during the joint closing. Note that the actual compressive strength of the example dam can be well in excess of 27.5 MPa (4,000 psi).

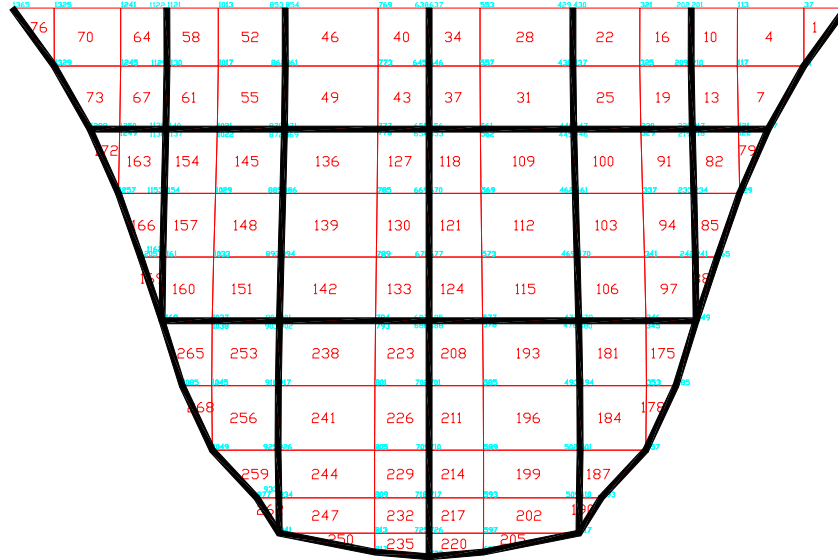


Figure F-22. Finite-element mesh with five vertical, two horizontal, and peripheral joints (Model 3)

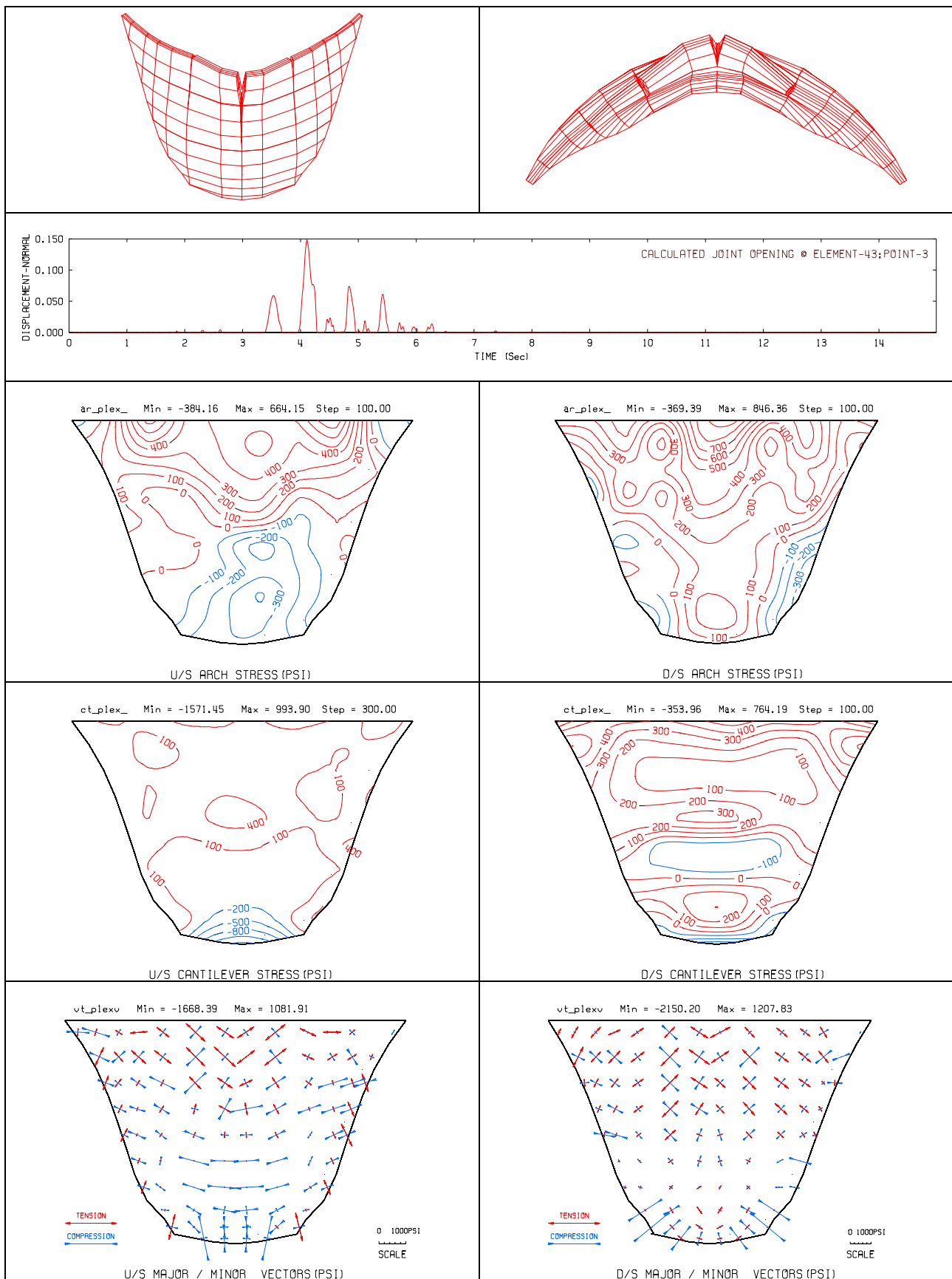


Figure F-23. Deflected shapes, maximum joint opening time history, envelopes of maximum arch and cantilever stresses, and envelopes of principal stress vectors due to CLD record

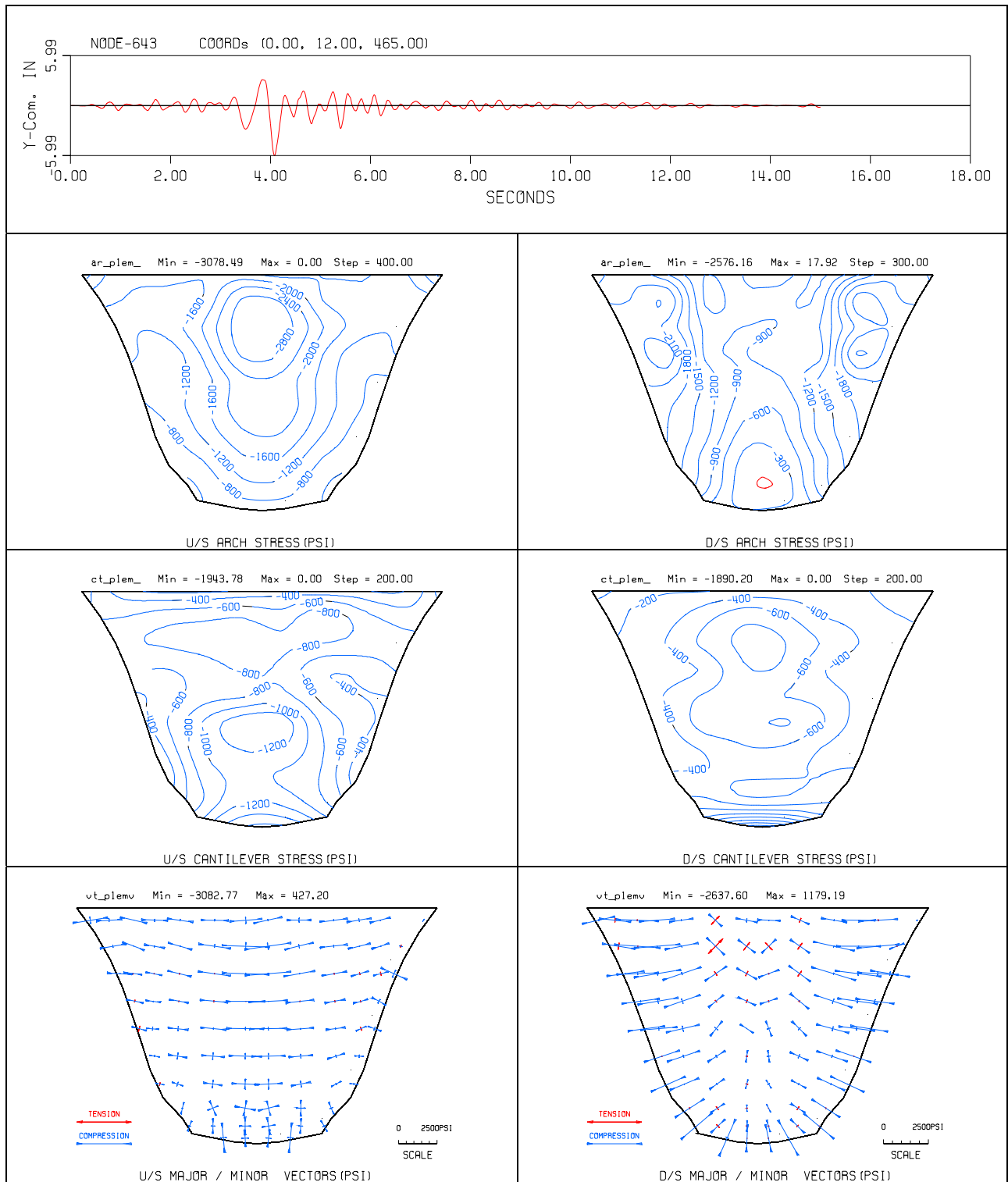


Figure F-23 (continued). Displacement time history, envelopes of minimum arch, cantilever, and principal stresses due to CLD record

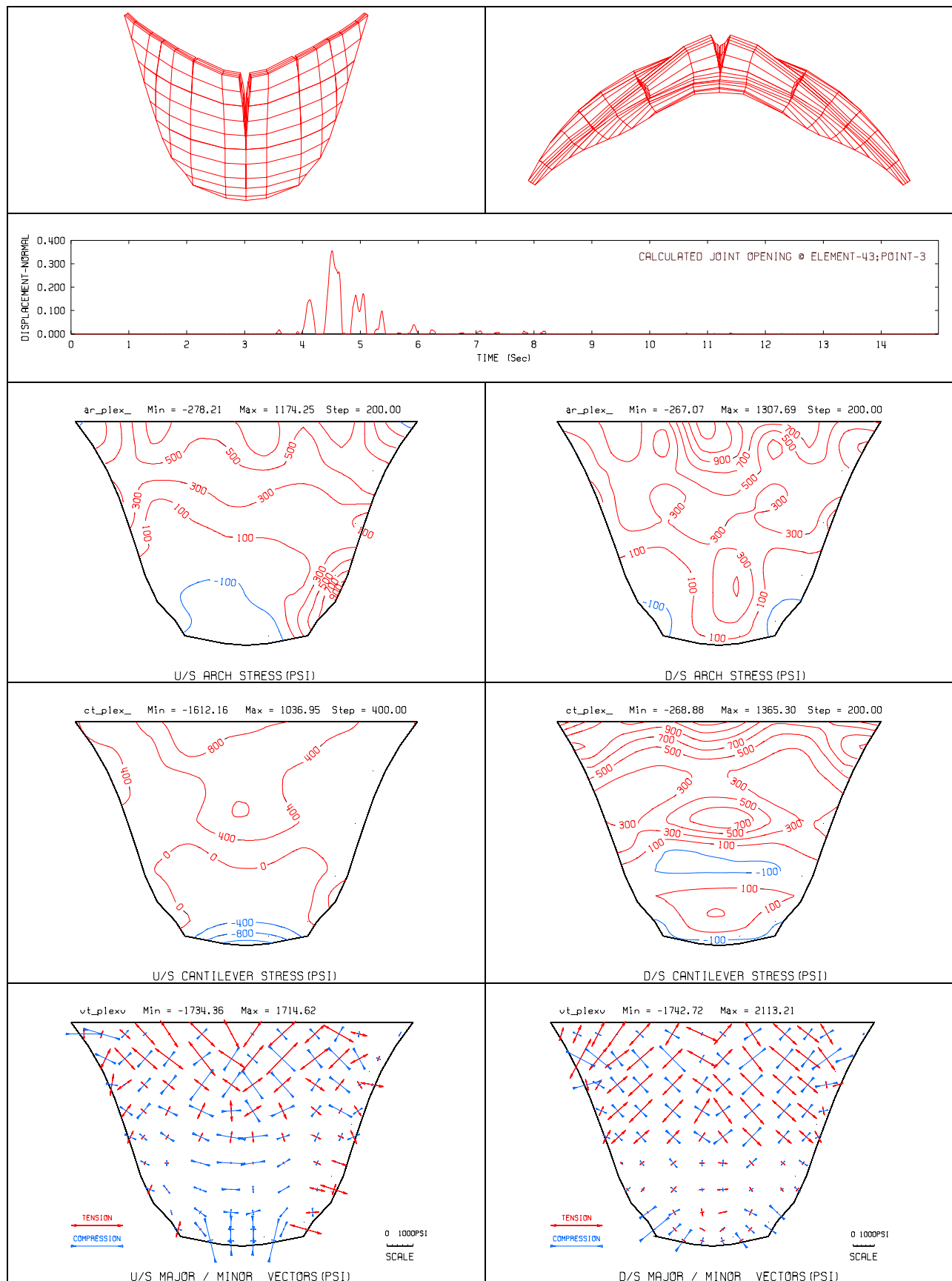


Figure F-24. Deflected shapes, maximum joint opening time history, envelopes of maximum arch and cantilever stresses, and envelopes of principal stress vectors due to GLY record

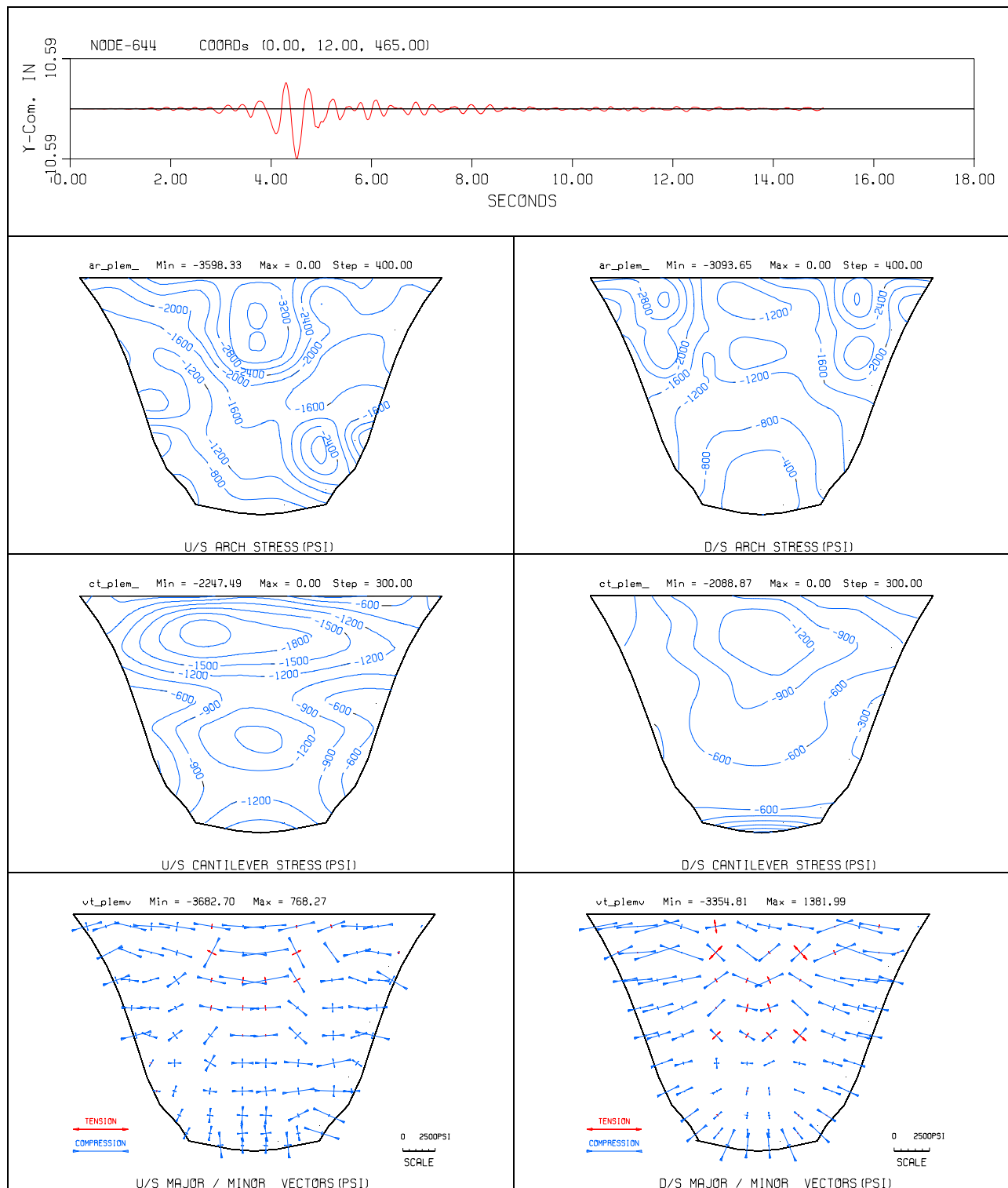


Figure F-24 (continued). Displacement time history, envelopes of minimum arch, cantilever, and principal stresses due to GLY record

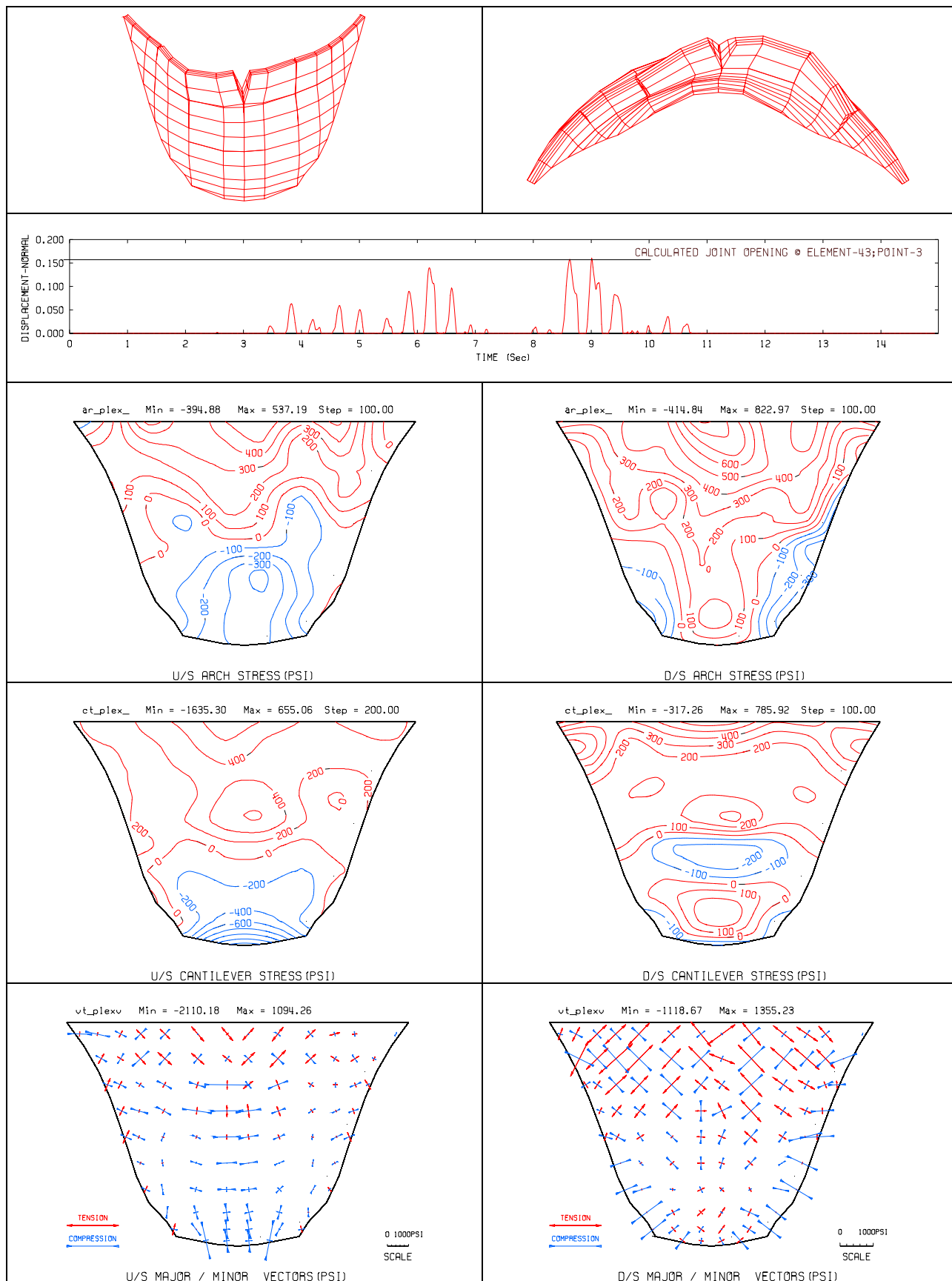


Figure F-25. Deflected shapes, maximum joint opening time history, envelopes of maximum arch and cantilever stresses, and envelopes of principal stress vectors due to PACB record

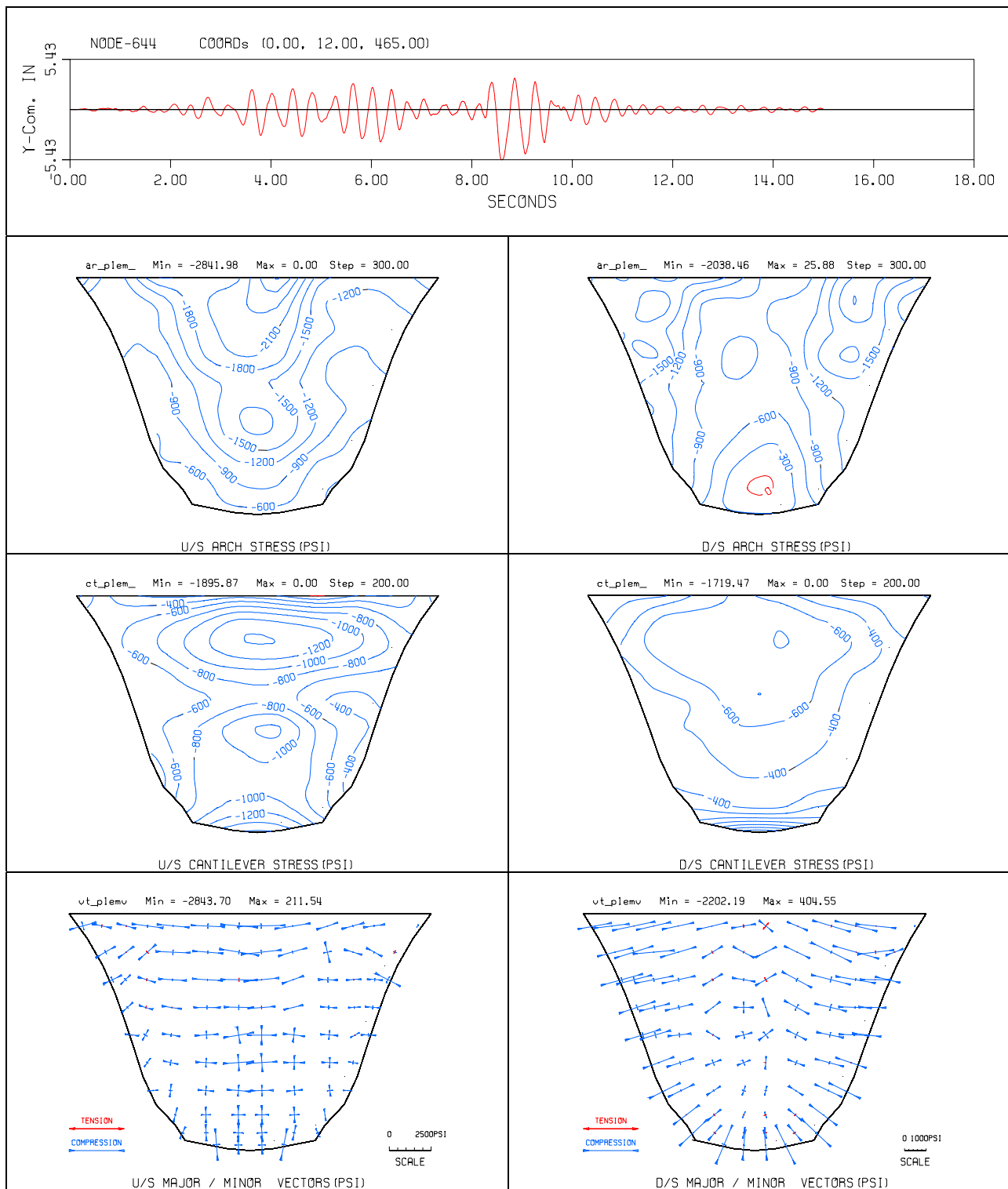


Figure F-25 (continued). Displacement time history, envelopes of minimum arch, cantilever, and principal stresses due to PACB record

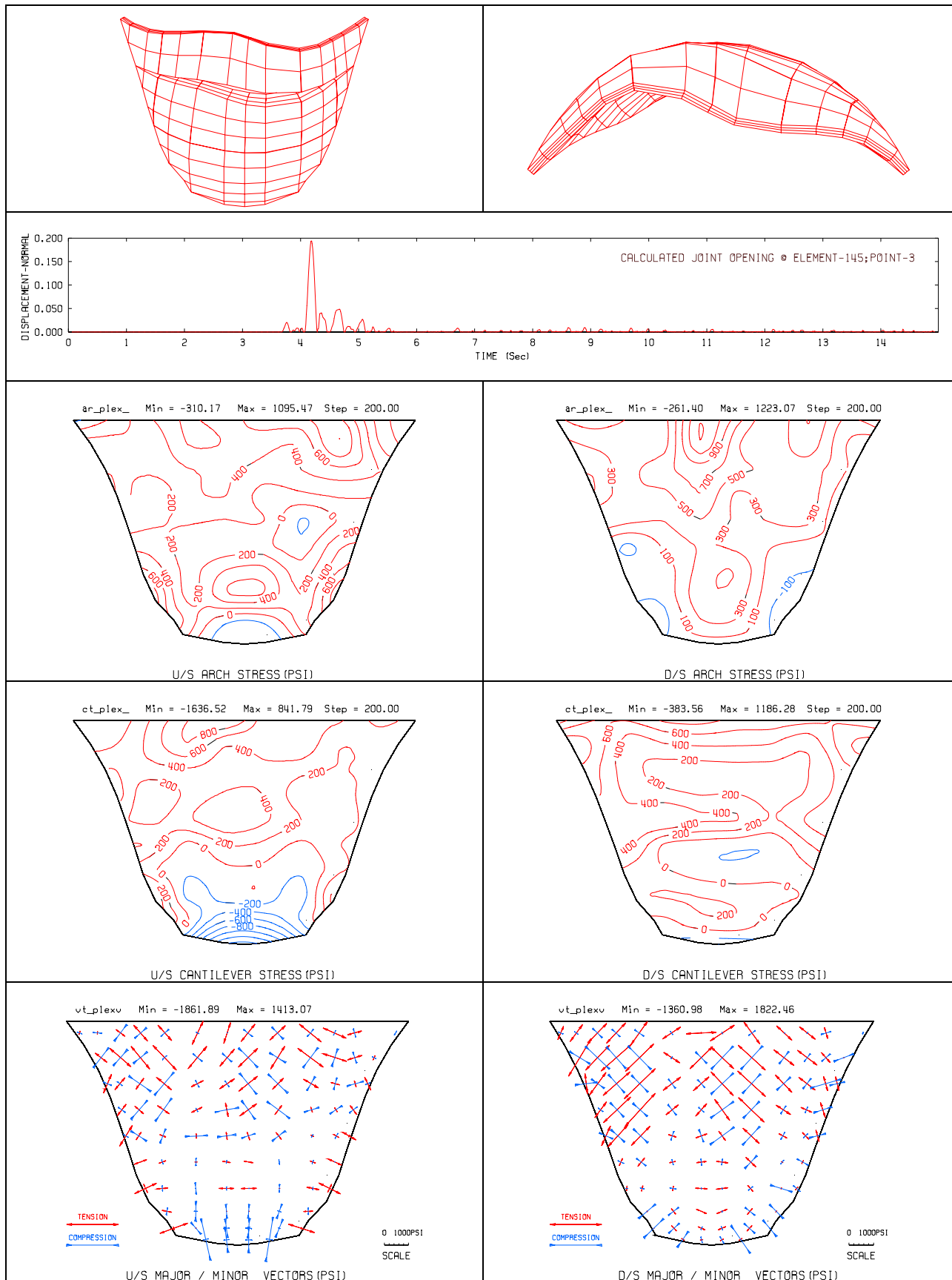


Figure F-26. Deflected shapes, maximum joint opening time history, envelopes of maximum arch and cantilever stresses, and envelopes of principal stress vectors due to PACN record

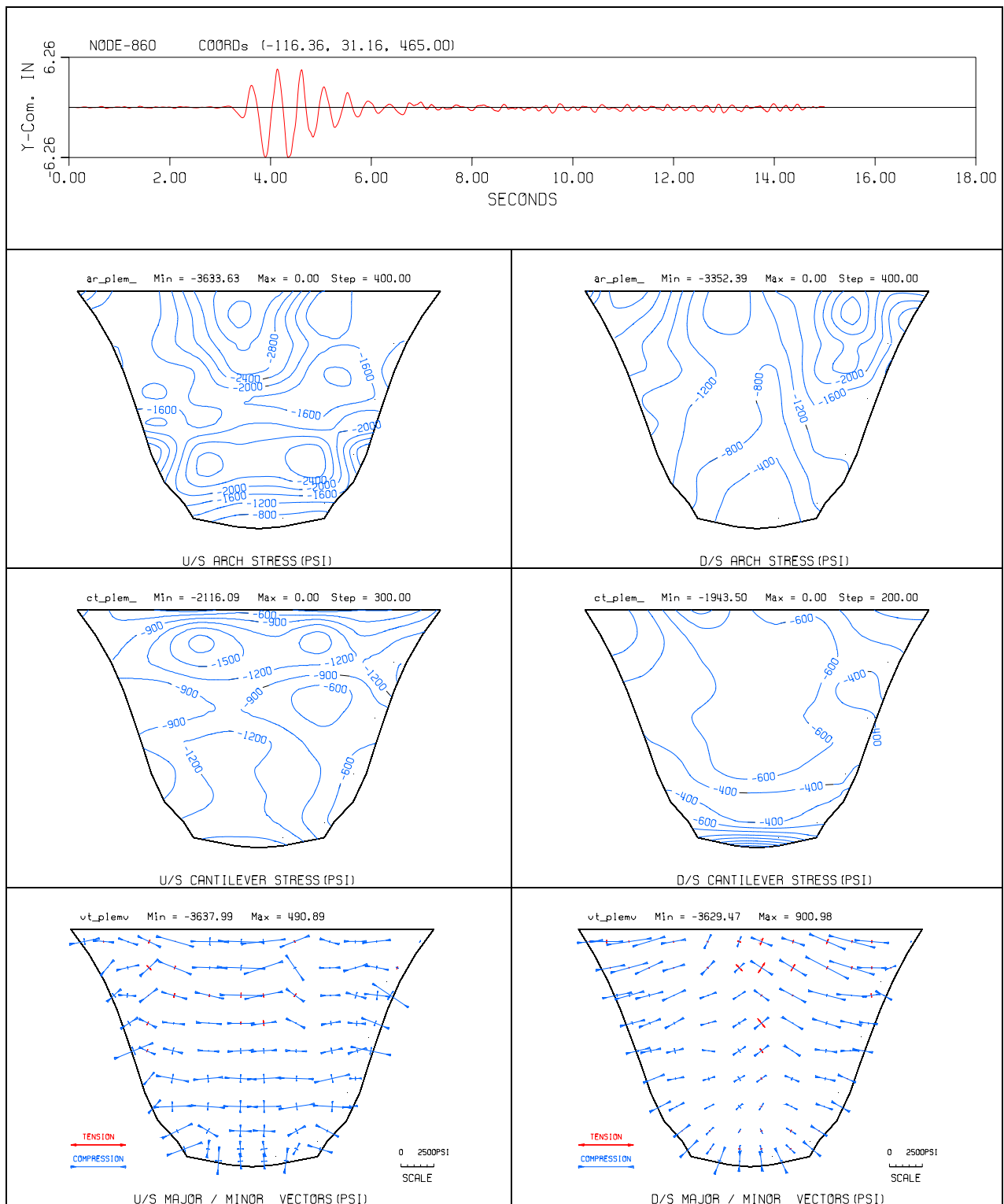


Figure F-26 (continued). Displacement time history, envelopes of minimum arch, cantilever, and principal stresses due to PACN record

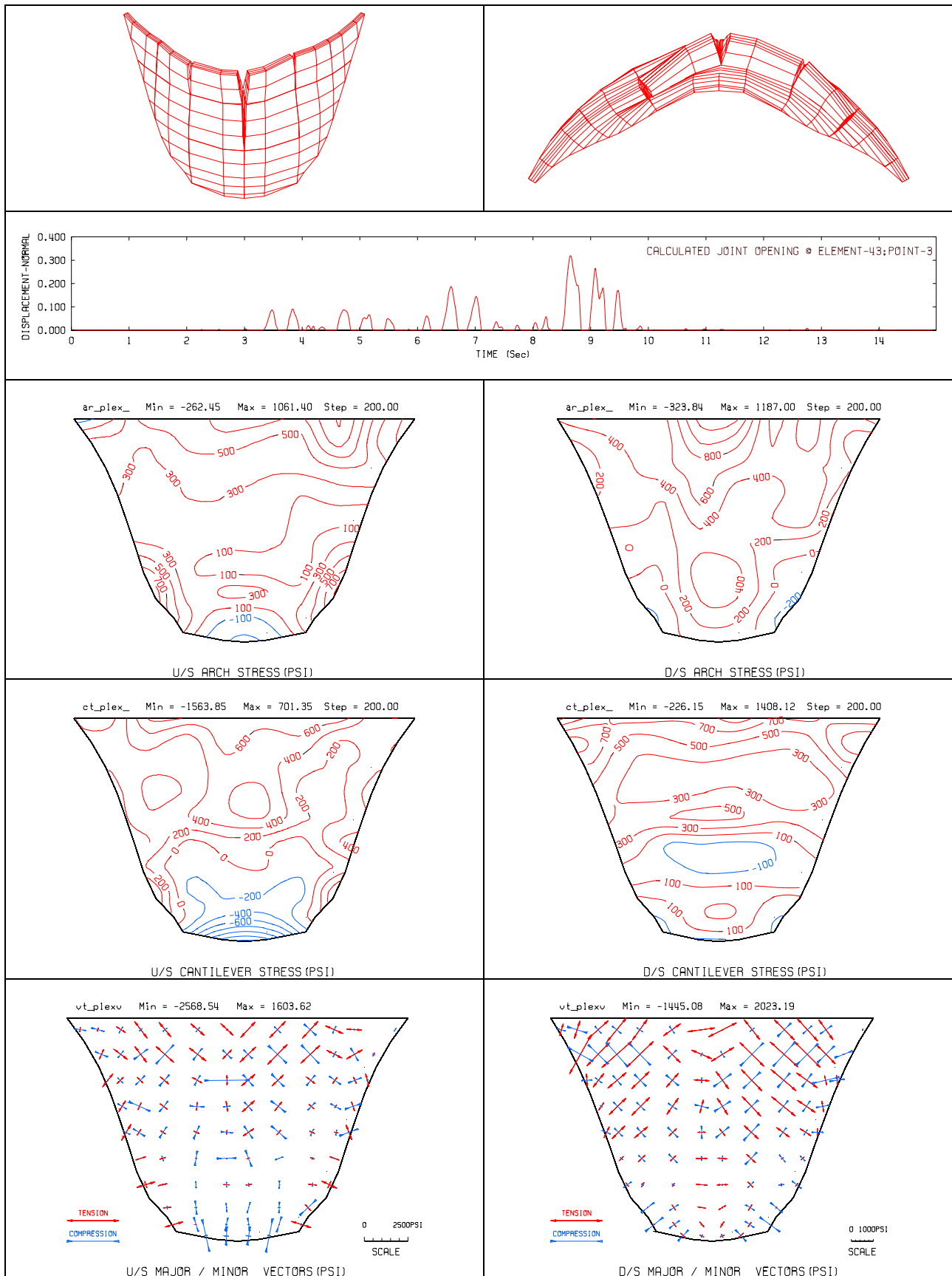


Figure F-27. Deflected shapes, maximum joint opening time history, envelopes of maximum arch and cantilever stresses, and envelopes of principal stress vectors due to PACX record

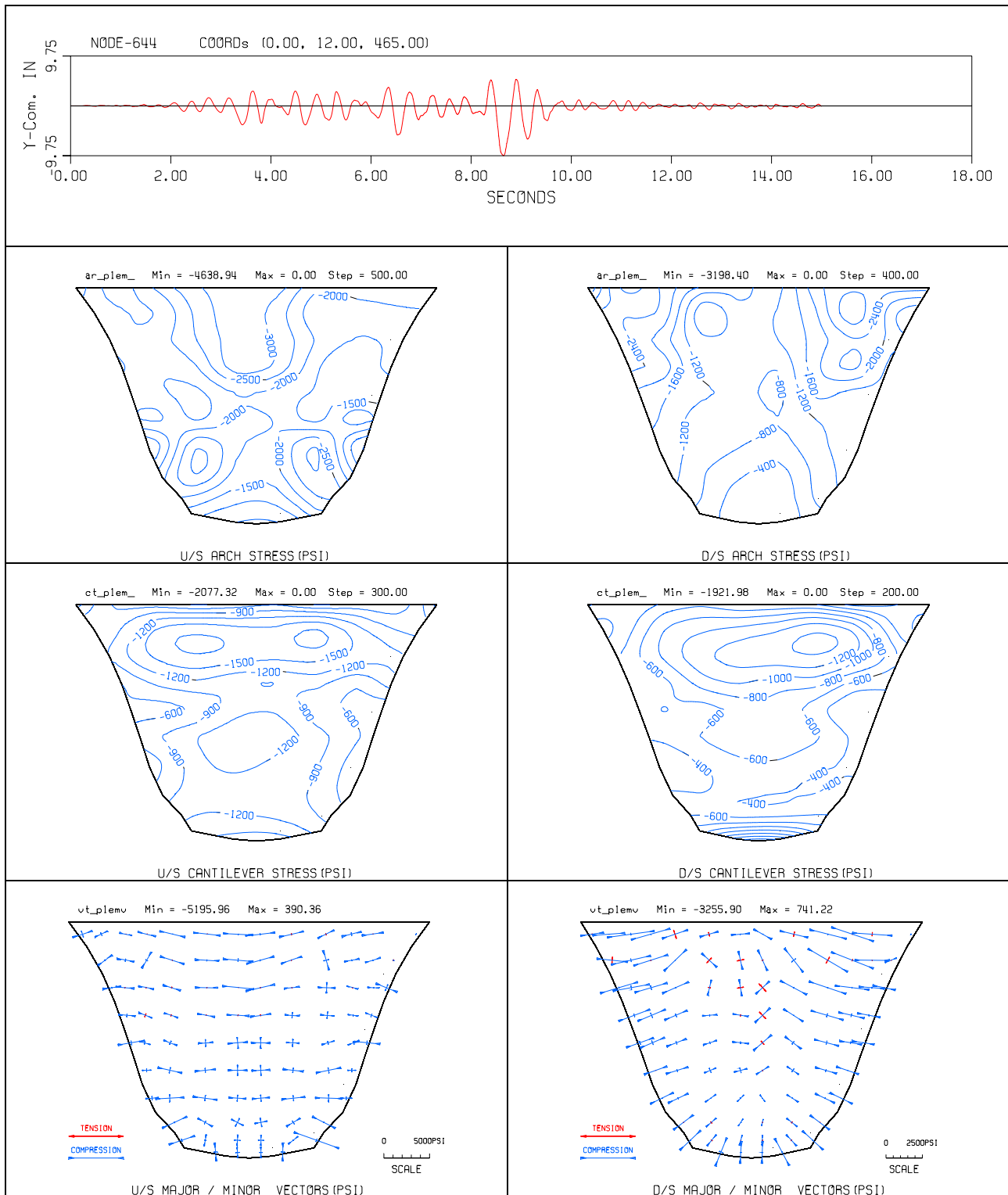


Figure F-27 (continued). Displacement time history, envelopes of minimum arch, cantilever, and principal stresses due to PACX record

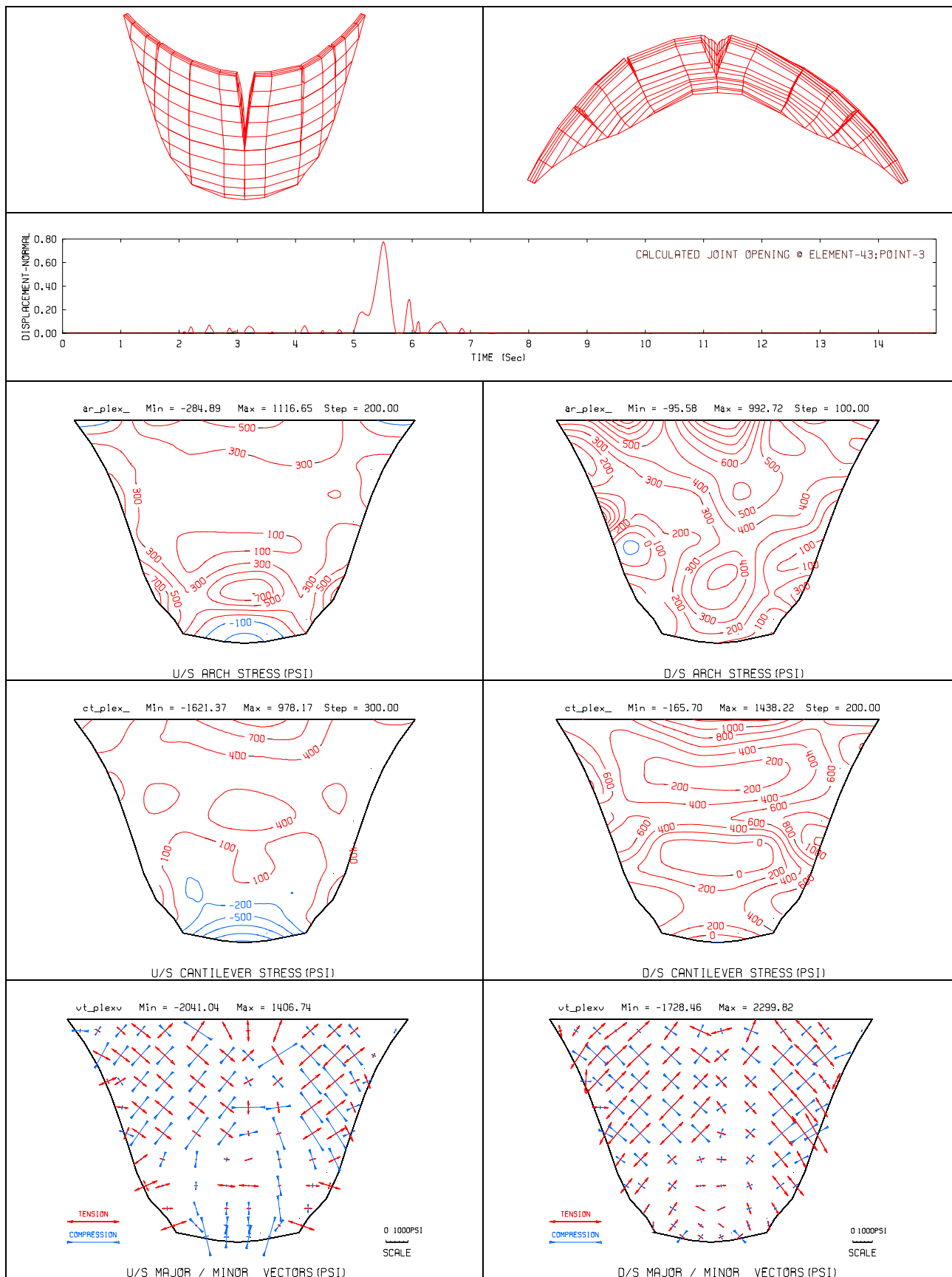


Figure F-28. Deflected shapes, maximum joint opening time history, envelopes of maximum arch and cantilever stresses, and envelopes of principal stress vectors due to U56 record

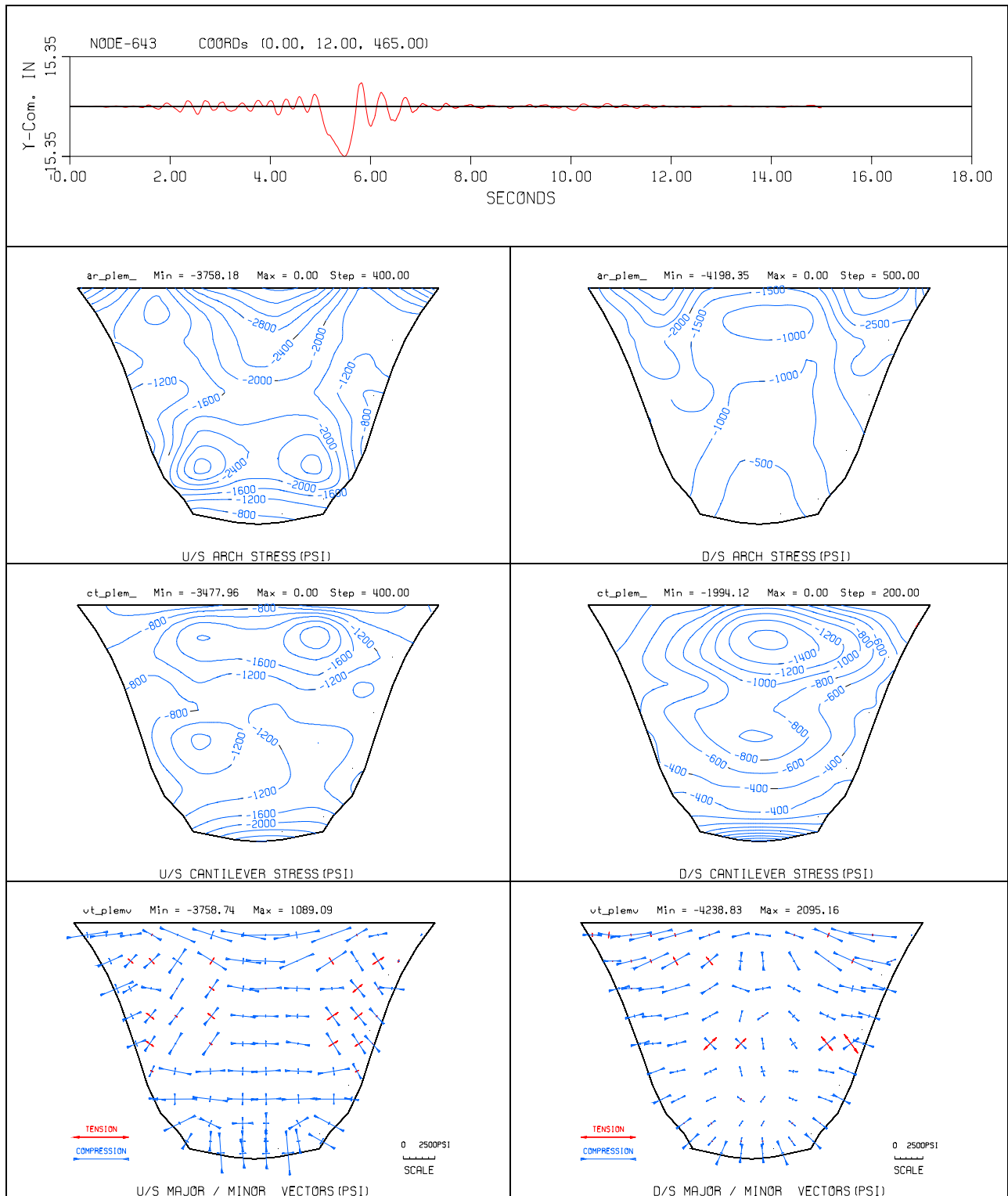


Figure F-28 (continued). Displacement time history, envelopes of minimum arch, cantilever, and principal stresses due to U56 record

## F-11. Evaluation of Results

Three finite-element models with three different joint configurations were analyzed using six different acceleration time histories representing a wide range of ground motion characteristics. Model-1 included three vertical contraction joints located at the crown section and at  $\frac{1}{4}$  span points of the dam. Model-2 consisted of five vertical contraction joints uniformly distributed across the length of the dam. Finally Model-3 incorporated five vertical, two horizontal, and the peripheral joints to allow for opening of the contraction joints and cracking/opening along the lift lines and the dam-foundation interface. The results for each model were tabulated and displayed in the form of deflected shapes, time-history of joint openings, stress contours, and the plots of principal stress vectors. Model-1 with three contraction joints indicated large joint opening at the crown section with high tensile arch and cantilever stresses still remaining within the cantilever blocks. Model-2 with five contraction joints was constructed to relieve the high tensile stresses by allowing a higher number of joints to open. The Model-2 results indicated only minor improvement, and high tensile stresses still persisted in the cantilever direction and at the dam-foundation interface. Model-3 was attempted to relief high tensile stresses by allowing two selected lift lines and the dam-foundation interface to open during the ground shaking. The amount of joint opening for Model-3 increased significantly for the Newhall record (U56) containing a one-second acceleration pulse. The significant increase in the amount of joint opening is attributed to the presence of the one-second acceleration pulse and partially free cantilever blocks formed in the upper part of the dam by two opened contraction joints on the sides and the opened lift line at the bottom of the blocks. Despite the significant joint opening, Model-3 still showed high tensile stresses within the cantilever blocks. This is believed to have been caused by the joint elements being constrained against tangential motion at the joint which did not permit joint slippage. The severity of the estimated joint opening is evaluated by comparing the amount of joint opening with the depth of shear keys to determine whether the blocks remain engaged through the shear keys. For this purpose snap shots of the maximum joint openings in the horizontal and vertical directions are shown in Figure F-29. The upper graph in this figure shows that the joint opening on the left side of the upper block (made of elements 28, 31, 34, and 37) exceeds the depth of shear key, but it is much smaller on the right side and bottom of the block. The lower graph in Figure F-29 shows that the amount of contraction joint openings at the time of the maximum lift line opening is much smaller than the depth of the shear keys. Overall, it appears that the upper blocks do not disengage from one another and more likely will remain stable. However, the stability condition should be confirmed by additional analyses that consider slippage across the contraction joints and lift lines which were ignored in this example. Furthermore other configuration of lift line openings should also be investigated.



**Figure F-29. Schematic view of estimated joint openings at the time of maximum horizontal joint opening (top) and at the time of maximum vertical joint opening (bottom)**

## F-12. Conclusions and Recommendations

a. *Conclusions.* The following conclusions are drawn from this nonlinear analysis example:

- (1) It is desirable to perform progressive evaluation of joint opening that starts with a minimum number of contraction joints and progresses by including more joints until realistic results are obtained.
- (2) Progressive evaluation of the results necessitates various joint configurations to be studied so that all potential joint-opening mechanisms are captured.
- (3) Inclusion of the contraction joints may not completely eliminate tensile stresses, although tensile stresses will be reduced. Allowing joint slippage should further reduce tensile stresses, if such capability is available.
- (4) Inclusion of the joints will increase time history displacements and compressive stresses. The resulting displacements and compressive stresses should be evaluated in assessment of the dam safety.

b. *Recommendations.* Based on the results of this example, the following recommendations are made regarding the nonlinear analysis procedures for arch dams:

- (1) Select a suite of six or more earthquake acceleration time histories for the analysis.
- (2) Perform linear-elastic time history analyses for all earthquakes input and evaluate the results according to the EM 1110-2-6053 performance criteria. If the linear-elastic performance criteria are not met, continue with nonlinear analyses.
- (3) Start the nonlinear analyses with a minimum number of three contraction joints. If dam experiences significant joint openings and large tensile stresses still persist, repeat the analysis with revised number of joints until realistic joint-opening mechanisms are achieved. The revised joint configuration may include vertical, horizontal, and peripheral joints.
- (4) Identify and conduct stability analyses for isolated blocks that may get loose and overtop as a result of excessive joint opening and lift line cracking.
- (5) Assess the overall safety of the dam with respect to structural stability and its ability to retain the impounded water.